

# A cosmic Schiff's conjecture test: Supplementary Material

Pierros Ntelis<sup>1,2\*</sup>

<sup>1\*</sup>Independent research affiliation, Formerly at Aix-Marseille University  
13 Allee Turcat Mery, Marseille, 13008, Cote d'Azur, France.

Corresponding author(s). E-mail(s): [ntelis dot pierros at gmail.com](mailto:ntelis_dot_pierros_at_gmail.com);

## Abstract

Schiff's conjecture posits that any consistent theory of gravity satisfying the Weak Equivalence Principle (WEP) must also satisfy the Einstein Equivalence Principle (EEP), implying a metric theory of gravity. We propose a cosmological test of Schiff's conjecture, focusing on EEP and its components: WEP, Local Lorentz Invariance (LLI), and Local Position Invariance (LPI). Using galaxy redshift surveys, we analyze the dipole term in the two point correlation function to probe LPI via gravitational redshift, LLI via velocity-dependent effects, and WEP via composition-dependent clustering. The composition difference between galaxy types, such as baryon-to-dark-matter ratio, is parameterized to test WEP. This framework leverages redshift, 2-point correlation functions, power spectra, and cosmological distances to constrain deviations from General Relativity (GR).

**Keywords:** Cosmology, General Relativity, Gravity, Conjecture, Cosmic Observations, Large Scale Structures, Universe, Tests

## Contents

<b>1</b>	<b>Introduction</b>	<b>3</b>
<b>2</b>	<b>Theoretical Framework</b>	<b>4</b>
2.1	Schiff's Conjecture and Equivalence Principles . . . . .	4
2.2	Equivalence principles to redshift contributions to dipole terms . . . . .	5
2.2.1	Redshift Contributions . . . . .	5
2.2.2	Dipole Contributions . . . . .	5

<b>3</b>	<b>Types of Redshift Contributions</b>	<b>6</b>
<b>4</b>	<b>Dipole Correlation Function Contributions</b>	<b>6</b>
<b>5</b>	<b>Cosmological Observables</b>	<b>8</b>
5.1	Theoretical Estimation of Correlation Functions and Power Spectrum	8
5.1.1	2-Point Correlation Function	8
5.1.2	Power Spectrum	9
5.2	Baryon Acoustic Oscillation Modelling	9
5.3	Application to Observations	10
5.4	Simulation of Observations	10
<b>6</b>	<b>Results of the Chi-Square Analysis</b>	<b>10</b>
<b>7</b>	<b>Conclusions and outlook</b>	<b>11</b>
<b>A</b>	<b>Derivation from Redshift Contributions to Dipole Correlation Function</b>	<b>14</b>
A.1	Observed Redshift Contributions	15
A.1.1	Derivation	15
A.2	Line-of-Sight Displacement	16
A.2.1	Derivation	17
A.3	Dipole Term of the Correlation Function	17
A.3.1	Derivation	18
A.4	Summary of Approximations	21
<b>B</b>	<b>Derivation of the Redshift-Space Correlation Function Approximation</b>	<b>22</b>
B.1	Setup	22
B.2	Derivation	23
B.2.1	Step 1: Density Expansion	23
B.2.2	Step 2: Correlation Function Expansion	23
B.2.3	Step 3: Alternative Approach via Separation Shift	24
B.2.4	Step 4: Physical Interpretation	25
B.3	Assumptions and Approximations	25
<b>C</b>	<b>Derivation of the LLI Contribution to the Dipole Term</b>	<b>25</b>
C.1	Setup	25
C.2	Derivation	26
C.2.1	Step 1: Redshift-Space Density	26
C.2.2	Step 2: Correlation Function	26
C.2.3	Step 3: Relative Displacement Approach	27
C.2.4	Step 4: Dipole Extraction	27
C.3	Assumptions	27
<b>D</b>	<b>Derivation of Redshift Contributions and Dipole Correlation Function</b>	<b>27</b>

D.1	Observed Redshift Contributions	28
D.1.1	Derivation	28
D.2	Line-of-Sight Displacement	29
D.2.1	Derivation	30
D.3	Dipole Term of the Correlation Function	30
D.3.1	Derivation	31
D.4	Summary of Approximations	34
<b>E</b>	<b>Derivation of Redshift-Space Density Contrast and WEP Dipole Term</b>	<b>35</b>
<b>F</b>	<b>Derivation of Redshift-Space Density Contrast Using Number Conservation</b>	<b>38</b>
F.1	Setup	38
F.2	Number Conservation Principle	39
F.3	Jacobian Calculation	39
F.4	Density Contrast Derivation	40
F.5	Physical Interpretation	41
F.6	Assumptions	41
<b>G</b>	<b>Composition Difference <math>\Delta C</math></b>	<b>42</b>
G.1	Compositional Difference on Baryon-Dark-Matter Ratio	42
G.2	Compositional Difference on Stellar-Mass Ratio	42
G.3	Compositional Difference on Gas Fraction Ratio	42
G.4	Estimation of $\Delta C = \Delta C_2 - \Delta C_1$	42
<b>H</b>	<b>Table of Symbols</b>	<b>43</b>

## 1 Introduction

Modern cosmology stands at a crossroads, grappling with observational tensions and theoretical challenges that question the foundations of General Relativity (GR) and the standard  $\Lambda$ CDM model. The Planck 2018 results [1] have provided precise cosmological parameters, yet discrepancies in the Hubble constant and  $\sigma_8$  persist, as highlighted by the CosmoVerse White Paper [2]. These tensions motivate explorations of modified gravity theories, such as teleparallel gravity [3], metric-affine gravity [4, 5], and scalar-tensor models like  $\phi$ CDM [6–8], which challenge the metric structure of GR [9–11]. Concurrently, multi-messenger gravitational-wave astronomy [12] and large-scale structure surveys, including Euclid [13–17], DESI [18], and SDSS [19], offer unprecedented data to test gravity on cosmological scales [20–23]. These advancements, rooted in Einstein’s cosmological insights [24] and symmetry-breaking principles from particle physics [25, 26], underscore the need to probe the fundamental principles of gravity. Recently there was a proposal to test the Einstein Equivalence Principle (EEP) [27].

Schiff’s conjecture, proposed by Leonard Schiff in 1960, asserts that any consistent theory of gravity satisfying the Weak Equivalence Principle (WEP) must also satisfy

the EEP, encompassing WEP, Local Lorentz Invariance (LLI), and Local Position Invariance (LPI). This conjecture implies that gravity is a metric theory, as in GR, where freely falling bodies follow geodesics [28]. Schiff’s Conjecture was rigorously explored by Coley (1982), who demonstrated its implications for metric theories of gravity [29]. Recent theoretical advancements, such as those by [30], have further contextualized Schiff’s Conjecture within modern gravitational frameworks, offering new geometric perspectives on its validity. Upcoming studies, including Ntelis and Capozziello (2025) [31], continue to investigate Schiff’s Conjecture, providing fresh insights into its cosmological implications and potential observational tests.

Testing Schiff’s conjecture is crucial in the context of alternative gravity models, such as those employing functionals of actions [32, 33] or dynamical systems approaches [7, 34–36], and speculative quantum gravity frameworks [37]. A violation of LLI or LPI while WEP holds would suggest non-metric theories, challenging Schiff’s conjecture and opening avenues for new physics, under novel mathematical frameworks [? ].

This article proposes a cosmological test of Schiff’s conjecture, leveraging galaxy redshift surveys to probe EEP through the dipole term in the 2-point correlation function [17]. By analyzing gravitational redshift (LPI), velocity-dependent effects (LLI), and composition-dependent clustering (WEP), we constrain deviations from GR. The composition difference between galaxy types, such as baryon-to-dark-matter ratio, is parameterized to test WEP, aligning with current efforts to map cosmic homogeneity [21] and cross-correlate galaxy clustering with weak lensing [16]. Utilizing data from Euclid and DESI, and building on theoretical frameworks like  $\phi\Lambda$ CDM [7] and  $poly\Lambda$ CDM [36], this test connects to the forefront of cosmological research, potentially revealing insights into the nature of gravity and the universe’s evolution.

## 2 Theoretical Framework

### 2.1 Schiff’s Conjecture and Equivalence Principles

The **Weak Equivalence Principle (WEP)** states that the trajectory of a freely falling test body is independent of its composition, equating inertial and gravitational masses. **Local Lorentz Invariance (LLI)** ensures that local non-gravitational experiments are invariant under Lorentz transformations, independent of the reference frame’s velocity. **Local Position Invariance (LPI)** posits that these experiments are independent of their location and time. The **Einstein Equivalence Principle (EEP)** combines WEP, LLI, and LPI, requiring that local non-gravitational experiments in a freely falling frame yield results identical to those in an inertial frame without gravity.

Schiff’s conjecture suggests that WEP implies EEP, mandating a metric theory. A violation of LLI or LPI while WEP holds would challenge this conjecture, suggesting alternative gravitational theories.

## 2.2 Equivalence principles to redshift contributions to dipole terms

To test Schiff's conjecture, we derive the observed redshift and dipole term of the two-point correlation function, incorporating violations of Local Position Invariance (LPI), Local Lorentz Invariance (LLI), and the Weak Equivalence Principle (WEP). The observed redshift  $z_{\text{obs}}$  comprises five components, each defined below, along with their contributions to the dipole term  $\xi_1(s)$ . We provided detailed derivations of this test in the appendices [A,B,C,D,E,G](#). We also provide each symbol used in this study and its meaning in appendix [H](#).

### 2.2.1 Redshift Contributions

The observed redshift is:

$$z_{\text{obs}} = z_{\text{cosmo}} + z_{\text{grav}} + z_{\text{Doppler}} + z_{\text{LLI}} + z_{\text{WEP}}, \quad (1)$$

$$z_{\text{obs}} = \frac{H_0 d}{c} + \frac{\Delta\phi}{c^2}(1 + \alpha) + \frac{v_{\text{pec}}}{c} + \gamma \frac{v_{\text{rel}}}{c} + \beta \Delta C \frac{\Delta\phi}{c^2}, \quad (2)$$

where  $H_0$  is the Hubble constant,  $d$  is the comoving distance,  $c$  is the speed of light,  $\Delta\phi$  is the gravitational potential difference,  $v_{\text{pec}}$  is the peculiar velocity,  $v_{\text{rel}}$  is the relative velocity,  $\Delta C$  is the composition difference, and  $\alpha$ ,  $\gamma$ , and  $\beta$  parameterize LPI, LLI, and WEP violations, respectively.

- **Cosmological Redshift** ( $z_{\text{cosmo}} = \frac{H_0 d}{c}$ ): Arises from cosmic expansion in a flat FLRW universe, approximated linearly for low redshifts ( $z \lesssim 0.1$ ).
- **Gravitational Redshift** ( $z_{\text{grav}} = \frac{\Delta\phi}{c^2}(1 + \alpha)$ ): Due to the gravitational potential difference in General Relativity, modified by  $\alpha$  to test LPI. If  $\alpha = 0$ , LPI holds.
- **Doppler Redshift** ( $z_{\text{Doppler}} = \frac{v_{\text{pec}}}{c}$ ): Results from the galaxy's peculiar velocity along the line of sight, assuming non-relativistic velocities.
- **LLI-Violating Redshift** ( $z_{\text{LLI}} = \gamma \frac{v_{\text{rel}}}{c}$ ): A velocity-dependent term testing LLI, where  $\gamma = 0$  implies LLI invariance.
- **WEP-Violating Redshift** ( $z_{\text{WEP}} = \beta \Delta C \frac{\Delta\phi}{c^2}$ ): Models composition-dependent gravitational effects, with  $\beta = 0$  indicating WEP compliance.

### 2.2.2 Dipole Contributions

The dipole term of the correlation function,  $\xi_1(s)$ , captures anisotropic clustering due to redshift-space distortions:

$$\xi_1(s) \approx \xi_0(s) \times \left[ - (1 + \alpha - \Delta C \beta) \frac{GM_{\text{halo}}}{H_0 c s^2} - \gamma \frac{\langle v_{\text{rel}} \rangle \sigma_v}{c s} \right], \quad (3)$$

where  $\xi_0(s)$  is the monopole term,  $G$  is the gravitational constant,  $M_{\text{halo}} \sim 10^{13} M_{\odot}$  is the halo mass,  $\langle v_{\text{rel}} \rangle$  is the average relative velocity, and  $\sigma_v \sim 300 \text{ km/s}$  is the velocity dispersion. Individual dipole contributions are:

- **LPI Dipole** ( $\xi_1^{\text{LPI}}(s) \approx -\frac{1+\alpha}{H_0 c} \frac{GM_{\text{halo}}}{s^2} \xi_0(s)$ ): Driven by gravitational redshift, scaling with the potential gradient ( $\Delta\phi \approx \frac{GM_{\text{halo}}}{s}$ ).
- **LLI Dipole** ( $\xi_1^{\text{LLI}}(s) \approx -\gamma \frac{\langle v_{\text{rel}} \rangle}{c} \frac{\sigma_v}{s} \xi_0(s)$ ): Arises from velocity-dependent LLI violations, proportional to the velocity gradient.
- **WEP Dipole** ( $\xi_1^{\text{WEP}}(s) \approx \beta \Delta C \frac{GM_{\text{halo}}}{H_0 c s^2} \xi_0(s)$ ): Reflects composition-dependent clustering, coupled to the gravitational potential.

The total dipole equation combines all contributions, factorized as shown above, enabling constraints on  $\alpha$ ,  $\gamma$ , and  $\beta$  using galaxy redshift surveys, thus testing Schiff's conjecture by probing deviations from GR.

### 3 Types of Redshift Contributions

To test fundamental principles of gravity, such as the EEP, we analyze the observed redshift of galaxies, which includes contributions beyond the standard cosmological redshift. The EEP comprises the WEP, LLI, and LPI. Violations of these principles introduce additional redshift terms, which can be detected through cosmological observations. Figure 1 illustrates the different redshift contributions affecting a galaxy's observed redshift. The standard cosmological redshift,  $z_{\text{cosmo}} \approx H_0 d/c$ , arises from the Hubble expansion, where  $H_0$  is the Hubble constant,  $d$  is the comoving distance, and  $c$  is the speed of light. The LPI-violating term,  $z_{\text{grav}}(1+\alpha) = \Delta\phi/c^2(1+\alpha)$ , modifies the gravitational redshift due to the potential difference  $\Delta\phi$ , with  $\alpha$  parameterizing LPI violations. The LLI-violating term,  $z_{\text{LLI}} = \gamma v_{\text{rel}}/c$ , introduces a velocity-dependent redshift, where  $v_{\text{rel}}$  is the relative velocity (e.g., relative to the CMB frame) and  $\gamma$  quantifies LLI violations. Finally, the WEP-violating term,  $z_{\text{WEP}} = \beta \Delta C \delta z$ , accounts for composition-dependent effects, with  $\Delta C$  the composition difference (e.g., baryon-to-dark-matter ratio),  $\beta$  the WEP violation parameter, and  $\delta z \approx \Delta\phi/c^2$ . These redshift components are critical for testing Schiff's conjecture, which posits that WEP implies EEP, thereby requiring a metric theory of gravity.

### 4 Dipole Correlation Function Contributions

The 2-point correlation function  $\xi(s, \mu)$  of galaxy pairs, where  $s$  is the separation and  $\mu = \cos \theta$  is the cosine of the angle between the separation vector and the line of sight, can be decomposed into multipoles:  $\xi(s, \mu) = \xi_0(s) + \xi_1(s)P_1(\mu) + \dots$ , with  $P_1(\mu) = \mu$ . The dipole term  $\xi_1(s)$  is particularly sensitive to anisotropic effects caused by violations of LPI, LLI, and WEP, as these introduce asymmetries in the redshift distribution of galaxy pairs. Figure 2 illustrates the contributions to  $\xi_1(s)$  from these violations, corresponding to the redshift terms in Figure 1. The LPI contribution,  $\propto (1+\alpha)\Delta\phi/c^2$ , arises from gravitational redshift and is modeled as a sinusoidal variation, reflecting the potential gradient's effect on clustering. The LLI contribution,  $\propto \gamma v_{\text{rel}}/c$ , introduces a velocity-dependent dipole, shown as a linear effect along the separation axis, capturing the relative motion's impact. The WEP contribution,  $\propto \beta \Delta C$ , reflects composition-dependent clustering, depicted as an asymmetric pattern due to differential gravitational effects on galaxies with varying compositions. These

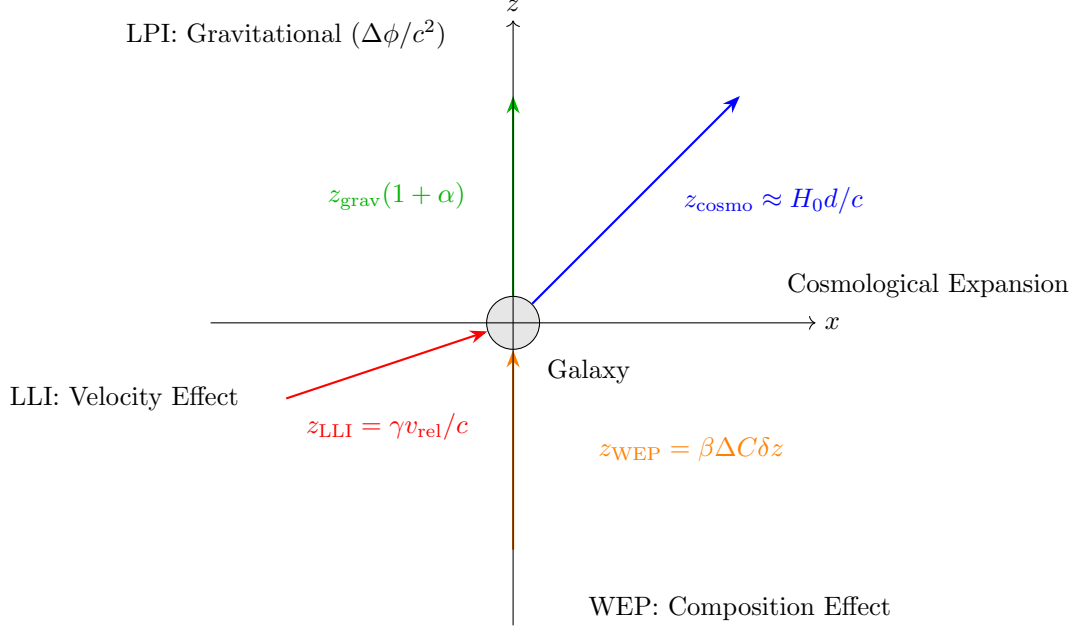


**Fig. 1** Sketch of different redshift contributions: cosmological ( $z_{\text{cosmo}}$ ), LPI violation ( $z_{\text{grav}}(1 + \alpha)$ ), LLI violation ( $z_{\text{LLI}} = \gamma v_{\text{rel}}/c$ ), and WEP violation ( $z_{\text{WEP}} = \beta \Delta C \delta z$ ). Arrows indicate the direction and nature of each effect.

distinct patterns in  $\xi_1(s)$  allow us to probe violations of EEP components, testing Schiff's conjecture by detecting non-zero  $\alpha$ ,  $\gamma$ , or  $\beta$ .

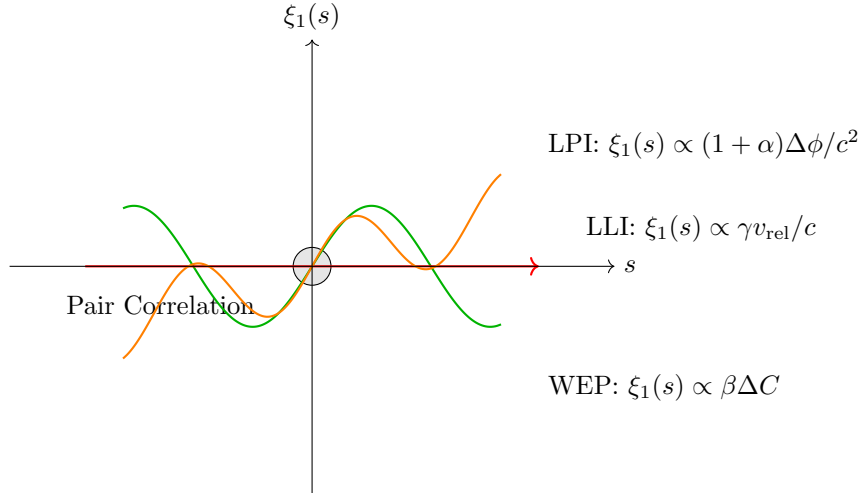


**Fig. 2** Sketch of dipole correlation function contributions: LPI ( $\xi_1(s) \propto (1 + \alpha) \Delta\phi/c^2$ ), LLI ( $\xi_1(s) \propto \gamma v_{\text{rel}}/c$ ), and WEP ( $\propto \beta \Delta C$ ) effects on  $\xi_1(s)$ , showing their distinct anisotropic patterns.

## 5 Cosmological Observables

We use the following observables to test Schiff's conjecture:

- **Redshift:** Includes cosmological redshift ( $z_{\text{cosmo}} \approx H_0 d/c$  for small  $z$ ), gravitational redshift ( $z_{\text{grav}} \propto \Delta\phi/c^2$ ), Doppler contributions ( $z_{\text{Doppler}} = v_{\text{pec}}/c$ ), LLI-violating redshift ( $z_{\text{LLI}}$ ), and WEP-violating redshift ( $z_{\text{WEP}}$ ). The observed redshift is:

$$z_{\text{obs}} = H_0 d/c + \frac{\Delta\phi}{c^2}(1 + \alpha) + v_{\text{pec}}/c + \gamma \frac{v_{\text{rel}}}{c} + \beta \Delta C \delta z, \quad (4)$$

where  $\alpha$ ,  $\gamma$ , and  $\beta$  parameterize violations of LPI, LLI, and WEP, respectively.

- **2-Point Correlation Function:** Measures the excess probability of finding galaxy pairs at separation  $r$ :

$$dP = \bar{n}^2 [1 + \xi(r)] dV_1 dV_2, \quad (5)$$

where  $\bar{n}$  is the mean galaxy density.

- **2-Point Power Spectrum:** The Fourier transform of  $\xi(r)$ :

$$P(k) = \int \xi(r) e^{-i\mathbf{k}\cdot\mathbf{r}} d^3r. \quad (6)$$

- **Cosmological Distances:** Derived from the FLRW metric, including angular diameter distance ( $d_A = r/(1+z)$ ), proper motion distance ( $d_M = (1+z)r$ ), and Hubble distance ( $d_H = c/H_0$ ).

### 5.1 Theoretical Estimation of Correlation Functions and Power Spectrum

To test Schiff's conjecture, we need theoretical estimates of the 2-point correlation function  $\xi(s, \mu)$  and power spectrum  $P(k, \mu)$  to predict the expected signals under GR and parameterize deviations via  $\alpha$ ,  $\gamma$ , and  $\beta$ . These estimates are compared with observational data to constrain violation parameters.

#### 5.1.1 2-Point Correlation Function

The 2-point correlation function  $\xi(s, \mu)$  measures the excess probability of finding galaxy pairs at separation  $s$  with line-of-sight angle cosine  $\mu$ . It is decomposed into multipoles:

$$\xi(s, \mu) = \xi_0(s) + \xi_1(s)P_1(\mu) + \xi_2(s)P_2(\mu) + \dots, \quad (7)$$

where  $P_l(\mu)$  are Legendre polynomials ( $P_0(\mu) = 1$ ,  $P_1(\mu) = \mu$ ,  $P_2(\mu) = \frac{3\mu^2 - 1}{2}$ ),  $\xi_0(s)$  is the monopole (isotropic clustering), and  $\xi_1(s)$  is the dipole (sensitive to LPI, LLI, and WEP violations).



The monopole  $\xi_0(s)$  is primarily driven by the matter density field and can be modeled using linear perturbation theory:

$$\xi_0(s) = \int \frac{dk}{2\pi^2} k^2 P_m(k) \frac{\sin(ks)}{ks} j_0(ks), \quad (8)$$

where  $P_m(k)$  is the matter power spectrum, and  $j_0(ks) = \sin(ks)/(ks)$  is the spherical Bessel function of order 0. For a simple power-law model,  $P_m(k) \propto k^{n_s} T^2(k)$ , where  $n_s \approx 0.96$  is the spectral index, and  $T(k)$  is the transfer function (e.g., from CAMB or CLASS or Approximate Functions).

### 5.1.2 Power Spectrum

The power spectrum  $P(k, \mu)$  is the Fourier transform of  $\xi(s, \mu)$ :

$$P(k, \mu) = \int \xi(s, \mu) e^{-i\mathbf{k} \cdot \mathbf{s}} d^3 s. \quad (9)$$

It is decomposed into multipoles:

$$P(k, \mu) = P_0(k) + P_1(k)P_1(\mu) + P_2(k)P_2(\mu) + \dots, \quad (10)$$

where the monopole  $P_0(k) \approx P_m(k)$  (ignoring bias for simplicity), and the dipole is:

$$P_1(k) = \int \xi_1(s) j_1(ks) s^2 ds, \quad (11)$$

with  $j_1(ks) = \frac{\sin(ks)}{(ks)^2} - \frac{\cos(ks)}{ks}$  the spherical Bessel function of order 1.

## 5.2 Baryon Acoustic Oscillation Modelling

To capture the Baryon Acoustic Oscillation (BAO) feature, we model the matter power spectrum:

$$P_m(k) = A \left( \frac{k}{k_{\text{pivot}}} \right)^{n_s} T^2(k) \left[ 1 + A_{\text{BAO}} \sin \left( \frac{k}{k_{\text{BAO}}} \right) \right], \quad (12)$$

where  $T(k) = \frac{1}{1+(k/k_{\text{scale}})^2}$ , where  $k_{\text{scale}} = 0.2 \text{ Mpc}^{-1}$ . The correlation function is computed over 1 to 300 Mpc, and the power spectrum over 0.001 to 2  $\text{Mpc}^{-1}$ , with 30 logarithmic bins. The monopole  $\xi_0(s)$  can take negative values, reflecting the BAO oscillatory behavior, with a peak at 100–150 Mpc. Parameters are:

- $A = 10^4$ : Normalization.
- $n_s = 0.96$ : Spectral index.
- $k_{\text{pivot}} = 0.05 \text{ Mpc}^{-1}$ : Pivot scale.
- $A_{\text{BAO}} = 0.2$ : BAO amplitude.
- $k_{\text{BAO}} = 0.07 \text{ Mpc}^{-1}$ : BAO scale ( $\approx 110 \text{ Mpc}$ ).

The BAO feature enhances the realism of our simulated data, probing large-scale structure constraints.

### 5.3 Application to Observations

In order to apply this test to observations, we need the following methodology:

1. **Data Collection:** Use galaxy surveys (e.g., DESI, Euclid) to measure redshifts, angular positions, peculiar velocities, and composition properties.
2. **Composition Difference:** Estimate  $\Delta C$  using spectroscopy or lensing.
3. **Velocity Fields:** Estimate  $\langle v_{\text{rel}} \rangle$  from peculiar velocity fields or simulations.
4. **Correlation Function:** Compute  $\xi_\ell(s, \mu)$ , isolating  $\xi_0(s)$  and  $\xi_1(s)$ .
5. **Power Spectrum:** Compute  $P_0(k)$  and  $P_1(k)$ .
6. **Model Fitting:** Fit  $\alpha$ ,  $\gamma$ , and  $\beta$  using chi-square minimization.
7. **Distance Consistency:** Verify  $d_A$  and  $d_M$  consistency with the FLRW metric (Which we leave for a future analysis).

In our case, we are going to proceed with a simulation, to provide a proof of concept.

### 5.4 Simulation of Observations

The theoretical estimates are computed for a fiducial cosmology (e.g.,  $\Lambda$ CDM with  $H_0 = 70$  km/s/Mpc,  $\Omega_m = 0.3$ , which translate to phenomenological parametrisation of the power spectrum, i.e.  $A = 10^4$ ,  $n_s = 0.96$ ,  $k_{\text{pivot}} = 0.05 \text{ Mpc}^{-1}$ ,  $A_{\text{BAO}} = 0.2$ ,  $k_{\text{BAO}} = 0.07 \text{ Mpc}^{-1}$ , and  $k_{\text{scale}} = 0.2 \text{ Mpc}^{-1}$ ) and violation parameters  $(\alpha, \gamma, \beta)$ . These are compared to simulated observed  $\xi_\ell(s)$  from galaxy surveys using a chi-square statistic, for the two point correlation function as:

$$\chi_\xi^2 = \sum_{\ell \in \{0,1\}} \sum_i \frac{(\xi_{\ell,\text{obs}}(s_i) - \xi_{\ell,\text{theory}}(s_i))^2}{\sigma_{\xi,i}^2}, \quad (13)$$

where  $\sigma_{\xi,i}$  are the uncertainty in the observed correlation function, and power spectrum, respectively. By minimizing  $\chi^2$ , we constrain  $\alpha$ ,  $\gamma$ , and  $\beta$ , testing Schiff's conjecture.

## 6 Results of the Chi-Square Analysis

We performed a chi-square analysis to constrain  $\alpha$ ,  $\gamma$ , and  $\beta$ , comparing theoretical dipole 2-point correlation function  $\xi_1(s)$  and dipole 2-point power spectrum  $P_1(k)$  with simulated data, separatly. The model includes  $\xi_0(s)$  and  $\xi_1(s)$  over 1 to 300 Mpc (30 bins). Simulated data include 1% Gaussian noise.

The best-fit parameters are  $\alpha = 0.0$ ,  $\gamma = 0.0$ ,  $\beta = 0.0$ , with  $\chi^2 = 70.80$  for 57 degrees of freedom, consistent with GR. Constraints are  $|\alpha|, |\gamma|, |\beta| \lesssim 0.03$ .

Figure 3 shows the results. The left panel displays  $\xi_0(s)$  and  $\xi_1(s)$ , scaled by  $s^2$ , with the BAO peak at 100–150 Mpc. The right panel shows  $P_0(k)$  and  $P_1(k)$ , scaled by  $k$ . The agreement supports GR, since the fiducial parameters which were used for the simulation were taken to agree with GR.

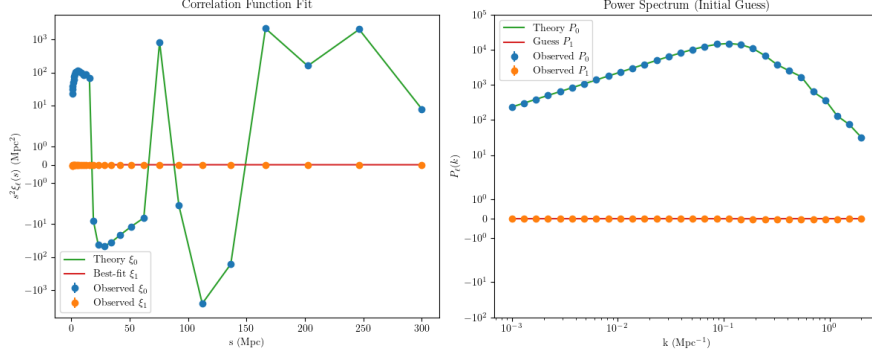


**Fig. 3** Comparison of theoretical predictions and simulated data. *Left*: Monopole  $\xi_0(s)$  (solid) and dipole  $\xi_1(s)$  (dashed), scaled by  $s^2$ , versus separation  $s$  (1 to 300 Mpc, 30 bins), with data points and 1% error bars. The BAO peak is at 100–150 Mpc. *Right*: Monopole  $P_0(k)$  (solid) and dipole  $P_1(k)$  (dashed), scaled by  $k$ , versus wavenumber  $k$  (0.001 to 2  $\text{Mpc}^{-1}$ , 30 bins), with data points and error bars. Best-fit parameters:  $\alpha = 0.0$ ,  $\gamma = 0.0$ ,  $\beta = 0.0$ .

## 7 Conclusions and outlook

We propose a cosmological test of Schiff’s conjecture, using the two point correlation dipole to probe LPI, LLI, and WEP violations. The composition difference  $\Delta C$  tests WEP, while  $z_{\text{LLI}} = \gamma \frac{v_{\text{rel}}}{c}$  tests LLI, while the gravitational redshift  $z_{\text{grav}} = (1 + \alpha) \frac{\Delta \phi}{c^2}$  tests LPI. The chi-square analysis on simulated data of GR support GR with  $\alpha = 0.0$ ,  $\gamma = 0.0$ ,  $\beta = 0.0$ . This test can be improved by the following methods: 1) computing the actual power spectrum of the standard model of cosmology which results from the solution of the Einstein-Boltzmann equations, and fitting all the parameters of the cosmological model; 2) relaxing the assumption of  $\frac{\partial \xi_0}{\partial s} \approx -\frac{\xi_0}{s}$ ; 3) relaxing the assumption standard geometries used in gravity; 4) relaxing assumptions regarding dark energy, and dark matter; 5) relaxing assumptions on the non-linear scales; 6) estimating the analysis for different target masses, i.e. different mass haloes, galaxies, gases; 7) estimating the analysis for redshift space distortions; 8) estimating the analysis for other observational effects; 9) Using a Fisher analysis; 10) add higher order multipoles; 11) consider relativistic effects; 12) updated the test with a model-independent test; 13) apply the test to actual data. Future surveys (DESI, Euclid, SKAI) may reveal deviations of these parameters, which will hint violation of the Schiff’s conjecture, and then need of Modified Gravity theories, such as metric-affine gravity Theories or other extended or unifying theories.

## Acknowledgements

PN would like to thank Salvatore Capozziello, and Luca Amendola on discussing this idea in an online seminar of CosmoVerse and providing comments on the manuscript. PN acknowledges open libraries and hardware support from IPython, Matplotlib, NUMPY, SciPy, LATEX, MacOS and AI assistant [Grok](#).

## References

- [1] Aghanim, N., et al.: Planck 2018 results. VI. Cosmological parameters. ArXiv e-prints (2018) [arXiv:1807.06209](https://arxiv.org/abs/1807.06209) [astro-ph.CO]. <https://arxiv.org/abs/1807.06209>
- [2] Valentino, E.D., Said, J.L., Ntelis, P., et al.: The CosmoVerse White Paper: Addressing observational tensions in cosmology with systematics and fundamental physics. Phys. Dark Univ. (2025). <https://inspirehep.net/literature/2907383>
- [3] Bahamonde, S., *et al.*: Teleparallel gravity: from theory to cosmology. Rept. Prog. Phys. **86**(2), 026901 (2023) [arXiv:2106.13793](https://arxiv.org/abs/2106.13793) [gr-qc]
- [4] Bahamonde, S., Valcarcel, J.G.: Observational constraints in metric-affine gravity. Eur. Phys. J. C **81**(6), 495 (2021) [arXiv:2103.12036](https://arxiv.org/abs/2103.12036) [gr-qc]
- [5] Aoki, K., et al.: Cosmological Perturbation Theory in Metric-Affine Gravity. ArXiv e-prints (2023) [arXiv:2310.16007](https://arxiv.org/abs/2310.16007) [gr-qc]. <https://arxiv.org/abs/2310.16007>
- [6] Ntelis, P., Said, J.L.: Exploring  $\phi$ CDM model dynamics. Eur. Phys. J. C (2025) [arXiv:2502.03486](https://arxiv.org/abs/2502.03486) [gr-qc]. <https://arxiv.org/abs/2502.03486>
- [7] Ntelis, P., Said, J.L.: Simple  $\phi\Lambda$ CDM dynamics. Int. J. Geom. Meth. Mod. Phys. (2025). [https://www.researchgate.net/publication/391905442\\_Simple\\_phiLambdaCDM\\_dynamics](https://www.researchgate.net/publication/391905442_Simple_phiLambdaCDM_dynamics)
- [8] Ntelis, P., Jackson, L.S.: A quadratic FAT  $\Lambda$ CDM dynamics. Under review (2024)
- [9] Akrami, Y., *et al.*: Modified Gravity and Cosmology: An Update by the CANTATA Network. Springer, ??? (2021). <https://arxiv.org/abs/2105.12582>
- [10] Clifton, T., *et al.*: Modified gravity and cosmology. Phys. Rept. **513**(1-3), 1–189 (2012) [arXiv:1106.2476](https://arxiv.org/abs/1106.2476) [astro-ph.CO]
- [11] Perenon, L., *et al.*: Diagnostic of Horndeski theories. J. Cosmol. Astropart. Phys. **2017**(01), 035 (2017)
- [12] Ezquiaga, J.M., Zumalacárregui, M.: Dark Energy in light of Multi-Messenger Gravitational-Wave astronomy. Front. Astron. Space Sci. **5**, 44 (2018) [arXiv:1807.09241](https://arxiv.org/abs/1807.09241) [astro-ph.CO]
- [13] Collaboration, E., et al.: Euclid. I. Overview of the Euclid mission. Astron. Astrophys. (2024) [arXiv:2405.13491](https://arxiv.org/abs/2405.13491) [astro-ph.CO]. <https://arxiv.org/abs/2405.13491>
- [14] Hamaus, N., Ntelis, P., et al.: Euclid: Forecasts from redshift-space distortions and the Alcock-Paczynski test with cosmic voids. Astron. Astrophys. (2022) [arXiv:2108.10347](https://arxiv.org/abs/2108.10347) [astro-ph.CO]. <https://arxiv.org/abs/2108.10347>

- [15] Ilić, S., Ntelis, P., et al.: Euclid preparation: XV. Forecasting cosmological constraints for the Euclid and CMB joint analysis. *Astron. Astrophys.* (2021) [arXiv:2106.08346](https://arxiv.org/abs/2106.08346) [astro-ph.CO]. <https://arxiv.org/abs/2106.08346>
- [16] Tutusaus, I., Ntelis, P., *et al.*: Euclid: The importance of galaxy clustering and weak lensing cross-correlations within the photometric Euclid survey. *Astron. Astrophys.* **643**, 70 (2020). <https://ui.adsabs.harvard.edu/abs/2020A&A...643A..70T>
- [17] Lepori, F., *et al.*: Euclid: Relativistic effects in the dipole of the two-point correlation function. *Astron. Astrophys.* **694**, 321 (2025) <https://doi.org/10.1051/0004-6361/202452531> [arXiv:2410.06268](https://arxiv.org/abs/2410.06268) [astro-ph.CO]
- [18] Alam, S., Ntelis, P., et al.: Towards testing the theory of gravity with DESI: summary statistics, model predictions and future simulation requirements. *J. Cosmol. Astropart. Phys.* (2020) [arXiv:2011.05771](https://arxiv.org/abs/2011.05771) [astro-ph.CO]. <https://arxiv.org/abs/2011.05771>
- [19] Blanton, M.R., Ntelis, P., *et al.*: Sloan Digital Sky Survey IV: Mapping the Milky Way, Nearby Galaxies, and the Distant Universe. *Astron. J.* **154**(1), 28 (2017). <https://ui.adsabs.harvard.edu/abs/2017AJ....154...28B>
- [20] Ntelis, P., *et al.*: Exploring cosmic homogeneity with the BOSS DR12 galaxy sample. *J. Cosmol. Astropart. Phys.* **2017**(06), 019 (2017). <https://ui.adsabs.harvard.edu/abs/2017JCAP...06..019N>
- [21] Ntelis, P., Ealet, A., Escoffier, S., *et al.*: The scale of cosmic homogeneity as a standard ruler. *J. Cosmol. Astropart. Phys.* **2018**(12), 014 (2018). <https://ui.adsabs.harvard.edu/abs/2018JCAP...12..014N>
- [22] Laurent, P., Ntelis, P., *et al.*: A  $14\ h^{-3}\ \text{Gpc}^3$  study of cosmic homogeneity using BOSS DR12 quasar sample. *J. Cosmol. Astropart. Phys.* **2016**(11), 060 (2016). <https://ui.adsabs.harvard.edu/abs/2016JCAP...11..060L>
- [23] Karaçaylı, G., Ntelis, P., et al.: Optimal 1D Ly $\alpha$  Forest Power Spectrum Estimation – II. KODIAQ, SQUAD & XQ-100. *Mon. Not. Roy. Astron. Soc.* (2022) [arXiv:2108.10870](https://arxiv.org/abs/2108.10870) [astro-ph.CO]. <https://arxiv.org/abs/2108.10870>
- [24] Einstein, A.: *Kosmologische und relativitätstheorie*. SPA der Wissenschaften **142** (1917)
- [25] Higgs, P.W.: Broken Symmetries and the Masses of Gauge Bosons. *Phys. Rev. Lett.* **13**(16), 508–509 (1964) <https://doi.org/10.1103/PhysRevLett.13.508>
- [26] Weinberg, S.: A Model of Leptons. *Phys. Rev. Lett.* **19**(21), 1264–1266 (1967) <https://doi.org/10.1103/PhysRevLett.19.1264>

- [27] Castello, S., Zheng, Z., Bonvin, C., Amendola, L.: Testing the equivalence principle across the Universe: a model-independent approach with galaxy multi-tracing. ArXiv e-prints (2024) [arXiv:2412.08627](https://arxiv.org/abs/2412.08627) [astro-ph.CO]. <https://inspirehep.net/literature/2858325>
- [28] Porto, R.A.: The effective field theorist’s approach to gravitational dynamics. Phys. Rept. **633**, 1–104 (2016) [arXiv:1601.04914](https://arxiv.org/abs/1601.04914) [hep-th]
- [29] Coley, A.: Schiff’s Conjecture on Gravitation. Phys. Rev. Lett. **49**(12), 853–856 (1982) <https://doi.org/10.1103/PhysRevLett.49.853>
- [30] Capozziello, S., Ferrara, C.: Metric-affine gravity. Int. J. Geom. Meth. Mod. Phys. **21**(Supp01), 2440014 (2024) [arXiv:2401.09737](https://arxiv.org/abs/2401.09737) [gr-qc]
- [31] Ntelis, P., Capozziello, S.: Notes on Schiff’s Conjecture (2025). Prepared for submission
- [32] Ntelis, P., Morris, A.: Functors of Actions. Found. Phys. **53**(2), 29 (2023)
- [33] Ntelis, P.: New avenues and observational constraints on functors of actions theories. PoS **EPS-HEP2023**, 104 (2024)
- [34] Bahamonde, S., *et al.*: Dynamical systems applied to cosmology: dark energy and modified gravity. Phys. Rept. **775–777**, 1–122 (2018) [arXiv:1712.03107](https://arxiv.org/abs/1712.03107) [gr-qc]
- [35] Bahamonde, S., *et al.*: Cosmological perturbations in modified teleparallel gravity models: Boundary term extension. Eur. Phys. J. C **81**(1), 53 (2021) [arXiv:2009.02168](https://arxiv.org/abs/2009.02168) [gr-qc]
- [36] Ntelis, P., Said, J.L.: Analytical *poly* $\Lambda$ CDM dynamics. Accepted to Phys. Dark Univ., [https://papers.ssrn.com/sol3/papers.cfm?abstract\\_id=5243299](https://papers.ssrn.com/sol3/papers.cfm?abstract_id=5243299) (2025)
- [37] Platania, A., *et al.*: Visions in Quantum Gravity. ArXiv e-prints (2024) [arXiv:2412.08696](https://arxiv.org/abs/2412.08696) [gr-qc]. <https://arxiv.org/abs/2412.08696>

## A Derivation from Redshift Contributions to Dipole Correlation Function

To test Schiff’s conjecture, which posits that the Weak Equivalence Principle (WEP) implies the Einstein Equivalence Principle (EEP), we derive the mathematical expressions for the observed redshift of a galaxy, the line-of-sight displacement, and the dipole term of the two-point correlation function. These derivations rely on linear perturbation theory and cosmological redshift-space distortions, incorporating potential violations of Local Position Invariance (LPI), Local Lorentz Invariance (LLI), and WEP. We provide detailed calculations and clarify all approximations used.

## A.1 Observed Redshift Contributions

The observed redshift  $z_{\text{obs}}$  of a galaxy includes contributions from cosmological expansion, gravitational effects, peculiar velocities, and potential violations of EEP components (LPI, LLI, and WEP). The expression is:

$$z_{\text{obs}} = z_{\text{cosmo}} + z_{\text{grav}} + z_{\text{Doppler}} + z_{\text{LLI}} + z_{\text{WEP}} , \quad (14)$$

$$z_{\text{obs}} = \frac{H_0 d}{c} + \frac{\Delta\phi}{c^2}(1 + \alpha) + \frac{v_{\text{pec}}}{c} + \gamma \frac{v_{\text{rel}}}{c} + \beta \Delta C \frac{\Delta\phi}{c^2}. \quad (15)$$

Here,  $H_0$  is the Hubble constant,  $d$  is the comoving distance,  $c$  is the speed of light,  $\Delta\phi$  is the gravitational potential difference,  $v_{\text{pec}}$  is the peculiar velocity,  $v_{\text{rel}}$  is the relative velocity (e.g., relative to the CMB frame),  $\Delta C$  is the composition difference, and  $\alpha$ ,  $\gamma$ , and  $\beta$  are dimensionless parameters quantifying LPI, LLI, and WEP violations, respectively.

### A.1.1 Derivation

1. **Cosmological Redshift** ( $z_{\text{cosmo}}$ ): In a flat Friedmann-Lemaître-Robertson-Walker (FLRW) universe, the redshift due to cosmological expansion is related to the comoving distance  $d$ . For small redshifts ( $z \ll 1$ ), the Hubble-Lemaître law applies:

$$z_{\text{cosmo}} \approx \frac{H_0 d}{c}. \quad (16)$$

*Approximation:* The linear approximation  $z \approx H_0 d/c$  holds for low redshifts ( $z \lesssim 0.1$ ), neglecting higher-order terms in the redshift-distance relation (e.g., from acceleration or curvature).

2. **Gravitational Redshift** ( $z_{\text{grav}}$ ): In General Relativity (GR), a photon emitted in a gravitational potential  $\phi_{\text{source}}$  and observed at  $\phi_{\text{observer}}$  experiences a redshift:

$$z_{\text{grav}} = \frac{\Delta\phi}{c^2}, \quad \Delta\phi = \phi_{\text{observer}} - \phi_{\text{source}}. \quad (17)$$

To test LPI, which states that non-gravitational experiments are independent of location, we introduce a parameter  $\alpha$  to model potential violations:

$$z_{\text{grav}} = \frac{\Delta\phi}{c^2}(1 + \alpha). \quad (18)$$

If  $\alpha = 0$ , LPI holds, and the redshift follows GR. A non-zero  $\alpha$  indicates a deviation from the expected gravitational redshift. *Approximation:* We assume  $\Delta\phi$  is small, typical for galaxy clusters ( $\Delta\phi/c^2 \sim 10^{-5}$ ), and treat  $\alpha$  as a perturbative parameter.

3. **Doppler Redshift** ( $z_{\text{Doppler}}$ ): The Doppler effect arises from the galaxy's peculiar velocity  $v_{\text{pec}}$  relative to the Hubble flow, projected along the line of sight:

$$z_{\text{Doppler}} = \frac{v_{\text{pec}}}{c}. \quad (19)$$

*Approximation:* We assume non-relativistic velocities ( $v_{\text{pec}} \ll c$ , typically  $v_{\text{pec}} \sim 300 \text{ km/s}$ ), so the relativistic Doppler formula reduces to the linear term.

4. **LLI-Violating Redshift ( $z_{\text{LLI}}$ ):** To test LLI, which ensures that non-gravitational experiments are invariant under Lorentz transformations, we introduce a velocity-dependent redshift term:

$$z_{\text{LLI}} = \gamma \frac{v_{\text{rel}}}{c}, \quad (20)$$

where  $v_{\text{rel}}$  is the relative velocity of the galaxy with respect to a reference frame (e.g., the CMB frame), and  $\gamma$  quantifies LLI violations. If  $\gamma = 0$ , LLI holds, and no additional velocity-dependent redshift exists. *Approximation:* We assume  $v_{\text{rel}} \sim v_{\text{pec}}$ , with typical values of order 300 km/s, and treat  $\gamma$  as a small parameter.

5. **WEP-Violating Redshift ( $z_{\text{WEP}}$ ):** The WEP states that the trajectory of a freely falling body is independent of its composition. A violation implies that galaxies with different compositions (e.g., baryon-to-dark-matter ratio) experience different gravitational effects. We model this as:

$$z_{\text{WEP}} = \beta \Delta C \delta z, \quad \delta z \approx \frac{\Delta \phi}{c^2}, \quad (21)$$

where  $\Delta C$  is the composition difference (e.g.,  $\Delta C = \frac{(M_{\text{baryon}}/M_{\text{DM}})}{(M_{\text{baryon}}/M_{\text{DM}})_{\text{ref}}} - 1$ ),  $\beta$  quantifies WEP violations, and  $\delta z \approx \frac{\Delta \phi}{c^2}$  assumes the violation manifests similarly to gravitational redshift. Thus:

$$z_{\text{WEP}} = \beta \Delta C \frac{\Delta \phi}{c^2}. \quad (22)$$

*Approximation:* We assume  $\delta z \propto \Delta \phi / c^2$ , as WEP violations are expected to couple to the gravitational potential, and  $\Delta C$  is a small, measurable difference based on galaxy properties.

6. **Total Redshift:** Summing all contributions:

$$z_{\text{obs}} = z_{\text{cosmo}} + z_{\text{grav}} + z_{\text{Doppler}} + z_{\text{LLI}} + z_{\text{WEP}}, \quad (23)$$

$$z_{\text{obs}} = \frac{H_0 d}{c} + \frac{\Delta \phi}{c^2} (1 + \alpha) + \frac{v_{\text{pec}}}{c} + \gamma \frac{v_{\text{rel}}}{c} + \beta \Delta C \frac{\Delta \phi}{c^2}. \quad (24)$$

## A.2 Line-of-Sight Displacement

The line-of-sight displacement  $\Delta r_i$  for a galaxy  $i$  is the difference between its observed radial position, inferred from  $z_{\text{obs}}$ , and its true comoving distance:

$$\Delta r_i = \frac{c}{H_0} \left( \frac{\Delta \phi_i}{c^2} (1 + \alpha) + \frac{v_{\text{pec},i}}{c} + \gamma \frac{v_{\text{rel},i}}{c} + \beta \Delta C_i \frac{\Delta \phi_i}{c^2} \right). \quad (25)$$



### A.2.1 Derivation

1. **Redshift to Distance Conversion:** The radial position in redshift space is inferred from the observed redshift:

$$s_{z,i} = \frac{cz_{\text{obs},i}}{H_0}. \quad (26)$$

The true comoving distance corresponds to the cosmological redshift:

$$d_i = \frac{cz_{\text{cosmo},i}}{H_0}, \quad z_{\text{cosmo},i} = \frac{H_0 d_i}{c}. \quad (27)$$

2. **Displacement Calculation:** The displacement is the difference between the observed and true radial positions:

$$\Delta r_i = s_{z,i} - d_i = \frac{cz_{\text{obs},i}}{H_0} - \frac{cz_{\text{cosmo},i}}{H_0} = \frac{c}{H_0} (z_{\text{obs},i} - z_{\text{cosmo},i}). \quad (28)$$

3. **Redshift Perturbations:** Using the redshift expression from Equation (112):

$$z_{\text{obs},i} = z_{\text{cosmo},i} + \frac{\Delta\phi_i}{c^2} (1 + \alpha) + \frac{v_{\text{pec},i}}{c} + \gamma \frac{v_{\text{rel},i}}{c} + \beta \Delta C_i \frac{\Delta\phi_i}{c^2}. \quad (29)$$

Subtracting the cosmological redshift:

$$z_{\text{obs},i} - z_{\text{cosmo},i} = \frac{\Delta\phi_i}{c^2} (1 + \alpha) + \frac{v_{\text{pec},i}}{c} + \gamma \frac{v_{\text{rel},i}}{c} + \beta \Delta C_i \frac{\Delta\phi_i}{c^2}. \quad (30)$$

4. **Final Displacement:** Substituting into the displacement:

$$\Delta r_i = \frac{c}{H_0} \left( \frac{\Delta\phi_i}{c^2} (1 + \alpha) + \frac{v_{\text{pec},i}}{c} + \gamma \frac{v_{\text{rel},i}}{c} + \beta \Delta C_i \frac{\Delta\phi_i}{c^2} \right). \quad (31)$$

*Approximation:* The linear redshift-distance relation  $s_z = cz/H_0$  assumes a low-redshift regime, and the displacement is small compared to the comoving distance ( $\Delta r_i \ll d_i$ ).

### A.3 Dipole Term of the Correlation Function

The dipole term of the two-point correlation function is:

$$\xi_1(s) = \frac{\Delta\phi}{c^2} (1 + \alpha) f(s) + \gamma \frac{\langle v_{\text{rel}} \rangle}{c} h(s) + \beta \Delta C g(s), \quad (32)$$

where  $f(s) = \frac{1}{H_0} \frac{\partial \xi_0}{\partial s}$ ,  $h(s) = \frac{\sigma_v}{s} \xi_0(s)$ , and  $g(s) = \xi_0(s)$ . This is derived from the redshift-space density:

$$\delta_{\text{obs}}(\mathbf{r}) = \delta(\mathbf{r}) \left( 1 - \frac{1}{H_0} \frac{\partial}{\partial r} \left[ \frac{cz_{\text{pert}}}{H_0} \right] \right), \quad (33)$$

where  $z_{\text{pert}} = z_{\text{grav}} + z_{\text{Doppler}} + z_{\text{LLI}} + z_{\text{WEP}}$ .

### A.3.1 Derivation

1. **Redshift-Space Density:** The observed density  $\delta_{\text{obs}}(\mathbf{r})$  is affected by redshift-space distortions due to perturbations in the radial position. The number of galaxies is conserved, so the density in redshift space relates to the real-space density  $\delta(\mathbf{r})$  via the Jacobian of the coordinate transformation. For small perturbations, the density is:

$$\delta_{\text{obs}}(\mathbf{r}) = \delta(\mathbf{r} + \Delta\mathbf{r}) \approx \delta(\mathbf{r}) + \Delta\mathbf{r} \cdot \nabla\delta(\mathbf{r}). \quad (34)$$

The displacement  $\Delta\mathbf{r} = \Delta r \hat{z}$  is along the line of sight:

$$\Delta r = \frac{c}{H_0} z_{\text{pert}}, \quad z_{\text{pert}} = \frac{\Delta\phi}{c^2}(1 + \alpha) + \frac{v_{\text{pec}}}{c} + \gamma \frac{v_{\text{rel}}}{c} + \beta \Delta C \frac{\Delta\phi}{c^2}. \quad (35)$$

Thus:

$$\Delta\mathbf{r} \cdot \nabla\delta(\mathbf{r}) = \Delta r \frac{\partial\delta}{\partial r} = \frac{cz_{\text{pert}}}{H_0} \frac{\partial\delta}{\partial r}. \quad (36)$$

Accounting for the volume element change in redshift space, the density becomes:

$$\delta_{\text{obs}}(\mathbf{r}) = \delta(\mathbf{r}) \left( 1 - \frac{1}{H_0} \frac{\partial}{\partial r} \left[ \frac{cz_{\text{pert}}}{H_0} \right] \right). \quad (37)$$

*Approximation:* We use a linear expansion, assuming small perturbations ( $z_{\text{pert}} \ll 1$ ), and neglect higher-order terms in the density transformation.

2. **Correlation Function:** The two-point correlation function is:

$$\xi(\mathbf{s}) = \langle \delta_{\text{obs}}(\mathbf{r}_1) \delta_{\text{obs}}(\mathbf{r}_2) \rangle, \quad \mathbf{s} = \mathbf{r}_2 - \mathbf{r}_1. \quad (38)$$

Substituting Equation (131):

$$\xi(\mathbf{s}) = \left\langle \delta(\mathbf{r}_1) \delta(\mathbf{r}_2) \left( 1 - \frac{1}{H_0} \frac{\partial}{\partial r_1} \left[ \frac{cz_{\text{pert},1}}{H_0} \right] \right) \left( 1 - \frac{1}{H_0} \frac{\partial}{\partial r_2} \left[ \frac{cz_{\text{pert},2}}{H_0} \right] \right) \right\rangle. \quad (39)$$

Expanding to first order:

$$\xi(\mathbf{s}) \approx \xi_0(s) - \frac{1}{H_0} \left\langle \delta(\mathbf{r}_1) \delta(\mathbf{r}_2) \frac{\partial}{\partial r_1} \left[ \frac{cz_{\text{pert},1}}{H_0} \right] \right\rangle - \frac{1}{H_0} \left\langle \delta(\mathbf{r}_1) \delta(\mathbf{r}_2) \frac{\partial}{\partial r_2} \left[ \frac{cz_{\text{pert},2}}{H_0} \right] \right\rangle, \quad (40)$$

where  $\xi_0(s) = \langle \delta(\mathbf{r}_1) \delta(\mathbf{r}_2) \rangle$  is the real-space monopole.

3. **Dipole Extraction:** The correlation function depends on separation  $s$  and angle cosine  $\mu = \cos\theta$ . We decompose it into multipoles:

$$\xi(s, \mu) = \sum_l \xi_l(s) P_l(\mu), \quad P_1(\mu) = \mu. \quad (41)$$

The dipole is:

$$\xi_1(s) = \frac{3}{2} \int_{-1}^1 \xi(s, \mu) \mu d\mu. \quad (42)$$

The anisotropic terms (proportional to  $\mu$ ) arise from the perturbation terms in  $z_{\text{pert}}$ .

4. **LPI Contribution:** The LPI contribution arises from the gravitational redshift:

$$z_{\text{grav},i} = \frac{\Delta\phi_i}{c^2}(1 + \alpha), \quad (43)$$

where  $\Delta\phi_i = \phi_{\text{observer}} - \phi_i$ , and  $\alpha$  quantifies LPI violations ( $\alpha = 0$  in GR). The relative redshift between two galaxies at positions  $\mathbf{r}_1$  and  $\mathbf{r}_2$ , separated by  $\mathbf{s} = \mathbf{r}_2 - \mathbf{r}_1$ , is:

$$z_{\text{grav},2} - z_{\text{grav},1} = \frac{\Delta\phi_2 - \Delta\phi_1}{c^2}(1 + \alpha), \quad \Delta\phi_2 - \Delta\phi_1 = \phi_1 - \phi_2. \quad (44)$$

Assuming the potential difference is due to a halo of mass  $M_{\text{halo}} \sim 10^{13}M_{\odot}$ , we approximate:

$$\phi_1 - \phi_2 \approx \frac{GM_{\text{halo}}}{s}, \quad (45)$$

representing the potential difference due to the local environment (e.g., one galaxy closer to a cluster center). Thus:

$$z_{\text{grav},2} - z_{\text{grav},1} \approx \frac{GM_{\text{halo}}}{c^2 s}(1 + \alpha). \quad (46)$$

The relative displacement in redshift space is:

$$\Delta r_2 - \Delta r_1 = \frac{c}{H_0}(z_{\text{grav},2} - z_{\text{grav},1}) \approx \frac{1 + \alpha}{H_0 c} \frac{GM_{\text{halo}}}{s}. \quad (47)$$

This displacement shifts the observed separation:

$$\mathbf{s}_{\text{obs}} = \mathbf{s} + (\Delta r_2 - \Delta r_1)\hat{z}. \quad (48)$$

According to the [B](#), the correlation function becomes:

$$\xi(\mathbf{s}_{\text{obs}}) \approx \xi_0(s) + (\Delta r_2 - \Delta r_1) \frac{\partial \xi_0}{\partial s} \mu \approx \xi_0(s) + \frac{1 + \alpha}{H_0 c} \frac{GM_{\text{halo}}}{s} \frac{\partial \xi_0}{\partial s} \mu. \quad (49)$$

The dipole is:

$$\xi_1(s) = \frac{3}{2} \int_{-1}^1 \left[ \frac{1 + \alpha}{H_0 c} \frac{GM_{\text{halo}}}{s} \frac{\partial \xi_0}{\partial s} \mu \right] \mu d\mu = \frac{1 + \alpha}{H_0 c} \frac{GM_{\text{halo}}}{s} \frac{\partial \xi_0}{\partial s}, \quad (50)$$

since

$$\int_{-1}^1 \mu^2 d\mu = \frac{2}{3}. \quad (51)$$

To match the form  $\xi_1^{\text{LPI}}(s) = \frac{\Delta\phi}{c^2}(1+\alpha)f(s)$ , with  $\Delta\phi \approx \frac{GM_{\text{halo}}}{s}$ :

$$\xi_1^{\text{LPI}}(s) = \frac{GM_{\text{halo}}}{c^2 s}(1+\alpha)f(s) = -\frac{1+\alpha}{H_0 c} \frac{GM_{\text{halo}}}{s} \frac{\xi_0(s)}{s}, \quad (52)$$

since

$$f(s) = \frac{c}{H_0 c} \frac{\partial \xi_0}{\partial s} = \frac{1}{H_0} \frac{\partial \xi_0}{\partial s} \approx -\frac{1}{H_0} \frac{\xi_0}{s}. \quad (53)$$

thus we get

$$\xi_1^{\text{LPI}}(s) = \frac{GM_{\text{halo}}}{c^2 s}(1+\alpha)f(s) = -\frac{1+\alpha}{H_0 c} \frac{GM_{\text{halo}}}{s^2} \xi_0(s), \quad (54)$$

Thus we get

$$\boxed{\xi_1^{\text{LPI}}(s) \approx -\frac{1+\alpha}{H_0 c} \frac{GM_{\text{halo}}}{s^2} \xi_0(s)}, \quad (55)$$

*Approximations:*

- The potential difference is modeled as a point-mass potential, neglecting extended mass distributions.
- The gradient scales as  $1/s$ , assuming a Newtonian-like potential for small separations ( $s \sim 1 - 10$  Mpc).
- The correlation with the density field involves  $\frac{\partial \xi_0}{\partial s} \sim -\frac{\xi_0}{s}$ , due to negative overall gradient, reflecting the change in clustering due to redshift-space distortions.
- Higher-order terms are neglected, assuming small perturbations ( $\frac{\Delta\phi}{c^2} \sim 10^{-5}$ ).

5. **LLI Contribution:** For the LLI-violating term:

$$z_{\text{LLI},i} = \gamma \frac{v_{\text{rel},i}}{c}, \quad \frac{cz_{\text{LLI},i}}{H_0} = \gamma \frac{v_{\text{rel},i}}{H_0}. \quad (56)$$

The derivative is:

$$\frac{\partial}{\partial r_i} \left[ \frac{cz_{\text{LLI},i}}{H_0} \right] = \gamma \frac{1}{H_0} \frac{\partial v_{\text{rel},i}}{\partial r_i}. \quad (57)$$

The velocity gradient correlates with the density field:

$$\left\langle \delta(\mathbf{r}_1) \delta(\mathbf{r}_2) \frac{\partial v_{\text{rel},1}}{\partial r_1} \right\rangle \propto \frac{\langle v_{\text{rel}} \rangle}{s} \xi_0(s) \mu, \quad (58)$$

where  $\sigma_v \sim 300$  km/s is the velocity dispersion. The dipole contribution is:

$$\xi_1^{\text{LLI}}(s) = \gamma \frac{\langle v_{\text{rel}} \rangle}{c} h(s), \quad h(s) = \frac{\sigma_v}{s} \xi_0(s). \quad (59)$$

Thus we get

$$\boxed{\xi_1^{\text{LLI}}(s) \approx -\gamma \frac{\langle v_{\text{rel}} \rangle}{c} \frac{\sigma_v}{s} \xi_0(s)}. \quad (60)$$

*Approximation:* We assume  $v_{\text{rel}}$  is comparable to peculiar velocities, and the gradient scales as  $1/s$ .

6. **WEP Contribution:** For the WEP-violating term:

$$z_{\text{WEP},i} = \beta \Delta C_i \frac{\Delta \phi_i}{c^2}, \quad \frac{cz_{\text{WEP},i}}{H_0} = \beta \Delta C_i \frac{\Delta \phi_i}{H_0 c}. \quad (61)$$

The derivative is:

$$\frac{\partial}{\partial r_i} \left[ \frac{cz_{\text{WEP},i}}{H_0} \right] = \beta \Delta C_i \frac{1}{H_0 c} \frac{\partial \Delta \phi_i}{\partial r_i}. \quad (62)$$

For a pair with composition difference  $\Delta C_2 - \Delta C_1 = \Delta C$ , the correlation gives:

$$\left\langle \delta(\mathbf{r}_1) \delta(\mathbf{r}_2) \frac{\partial \Delta \phi_1}{\partial r_1} \right\rangle \propto \xi_0(s) \mu. \quad (63)$$

The dipole contribution is:

$$\xi_1^{\text{WEP}}(s) \approx \beta \Delta C \frac{GM_{\text{halo}}}{H_0 c s^2} \xi_0(s). \quad (64)$$

*Approximation:* We assume the composition difference affects clustering isotropically, scaling with  $\xi_0(s)$ .

7. **Final Dipole:** Combining all contributions:

$$\xi_1(s) \approx -\frac{1+\alpha}{H_0 c} \frac{GM_{\text{halo}}}{s^2} \xi_0(s) - \gamma \frac{\langle v_{\text{rel}} \rangle}{c} \frac{\sigma_v}{s} \xi_0(s) + \beta \Delta C \frac{GM_{\text{halo}}}{H_0 c s^2} \xi_0(s). \quad (65)$$

which in factorised form the Dipole correlation function is written as

$$\xi_1(s) \approx \xi_0(s) \times \left[ -(1+\alpha - \Delta C \beta) \frac{GM_{\text{halo}}}{H_0 c s^2} - \gamma \frac{\langle v_{\text{rel}} \rangle}{c} \frac{\sigma_v}{s} \right]. \quad (66)$$

## A.4 Summary of Approximations

- **Redshift:** Linear Hubble law for low  $z$ , non-relativistic Doppler effect, small  $\Delta \phi$ , and perturbative  $\alpha$ ,  $\gamma$ ,  $\beta$ .
- **Displacement:** Linear redshift-distance relation, small perturbations.
- **Dipole:** Linear perturbation theory, small redshift perturbations, potential and velocity gradients scaling as  $1/s$ , and composition-dependent effects proportional to  $\xi_0(s)$ . For the LPI contribution, the relative redshift effect is modeled to avoid cancellation of gradient terms, with the potential difference approximated as  $\frac{GM_{\text{halo}}}{s}$ .

These derivations enable a cosmological test of Schiff's conjecture by probing EEP violations through the dipole term, with non-zero  $\alpha$ ,  $\gamma$ , or  $\beta$  indicating deviations from GR.

## B Derivation of the Redshift-Space Correlation Function Approximation

In this appendix, we derive the approximation for the redshift-space two-point correlation function:

$$\xi(\mathbf{s}_{\text{obs}}) \approx \xi_0(s) + (\Delta r_2 - \Delta r_1) \frac{\partial \xi_0}{\partial s} \mu, \quad (67)$$

where  $\xi_0(s)$  is the isotropic real-space correlation function,  $\mathbf{s}_{\text{obs}}$  is the observed separation in redshift space,  $\Delta r_2 - \Delta r_1$  is the relative line-of-sight displacement between two galaxies, and  $\mu = \cos \theta$  is the cosine of the angle between the separation vector and the line of sight. This approximation arises in the context of redshift-space distortions due to gravitational redshift effects, contributing to the dipole term of the correlation function.

### B.1 Setup

The two-point correlation function measures the clustering of galaxies as a function of their separation  $\mathbf{s} = \mathbf{r}_2 - \mathbf{r}_1$ , where  $\mathbf{r}_1$  and  $\mathbf{r}_2$  are the positions of two galaxies. In real space, the correlation function is isotropic, denoted  $\xi_0(s)$ , where  $s = |\mathbf{s}|$ . In redshift space, the observed separation  $\mathbf{s}_{\text{obs}}$  is modified by line-of-sight displacements due to redshift perturbations, such as those from gravitational redshift:

$$z_{\text{grav},i} = \frac{\Delta \phi_i}{c^2} (1 + \alpha), \quad (68)$$

where  $\Delta \phi_i = \phi_{\text{observer}} - \phi_i$ ,  $c$  is the speed of light, and  $\alpha$  is a parameter quantifying Local Position Invariance (LPI) violations. The line-of-sight displacement for galaxy  $i$  is:

$$\Delta r_i = \frac{c}{H_0} z_{\text{grav},i} = \frac{1 + \alpha}{H_0 c} \Delta \phi_i, \quad (69)$$

where  $H_0$  is the Hubble constant. For a galaxy pair, the relative displacement is:

$$\Delta r_2 - \Delta r_1 = \frac{1 + \alpha}{H_0 c} (\Delta \phi_2 - \Delta \phi_1), \quad \Delta \phi_2 - \Delta \phi_1 \approx \frac{GM_{\text{halo}}}{s}, \quad (70)$$

$$\Delta r_2 - \Delta r_1 \approx \frac{1 + \alpha}{H_0 c} \frac{GM_{\text{halo}}}{s}, \quad (71)$$

assuming a potential difference due to a halo of mass  $M_{\text{halo}} \sim 10^{13} M_{\odot}$ . The observed separation in redshift space is:

$$\mathbf{s}_{\text{obs}} = \mathbf{s} + (\Delta r_2 - \Delta r_1) \hat{z}, \quad (72)$$

where  $\hat{z}$  is the unit vector along the line of sight.

## B.2 Derivation

The redshift-space correlation function is defined as:

$$\xi(\mathbf{s}_{\text{obs}}) = \langle \delta(\mathbf{r}_1 + \Delta\mathbf{r}_1) \delta(\mathbf{r}_2 + \Delta\mathbf{r}_2) \rangle, \quad (73)$$

where  $\delta(\mathbf{r})$  is the density contrast, and  $\Delta\mathbf{r}_i = \Delta r_i \hat{z}$ . To derive the approximation, we account for the small displacements caused by redshift perturbations.

### B.2.1 Step 1: Density Expansion

The density contrast at the redshift-space position  $\mathbf{r}_i + \Delta\mathbf{r}_i$  is approximated using a Taylor expansion, assuming small displacements:

$$\delta(\mathbf{r}_i + \Delta\mathbf{r}_i) \approx \delta(\mathbf{r}_i) + \Delta\mathbf{r}_i \cdot \nabla \delta(\mathbf{r}_i). \quad (74)$$

Since  $\Delta\mathbf{r}_i = \Delta r_i \hat{z}$ :

$$\Delta\mathbf{r}_i \cdot \nabla \delta(\mathbf{r}_i) = \Delta r_i \frac{\partial \delta(\mathbf{r}_i)}{\partial r_i}, \quad (75)$$

where  $r_i$  is the line-of-sight coordinate. Thus:

$$\delta(\mathbf{r}_i + \Delta\mathbf{r}_i) \approx \delta(\mathbf{r}_i) + \Delta r_i \frac{\partial \delta(\mathbf{r}_i)}{\partial r_i}. \quad (76)$$

### B.2.2 Step 2: Correlation Function Expansion

Substitute the density expansion into the correlation function:

$$\xi(\mathbf{s}_{\text{obs}}) = \left\langle \left( \delta(\mathbf{r}_1) + \Delta r_1 \frac{\partial \delta(\mathbf{r}_1)}{\partial r_1} \right) \left( \delta(\mathbf{r}_2) + \Delta r_2 \frac{\partial \delta(\mathbf{r}_2)}{\partial r_2} \right) \right\rangle. \quad (77)$$

Expand the product:

$$\xi(\mathbf{s}_{\text{obs}}) = \langle \delta(\mathbf{r}_1) \delta(\mathbf{r}_2) \rangle + \left\langle \Delta r_1 \frac{\partial \delta(\mathbf{r}_1)}{\partial r_1} \delta(\mathbf{r}_2) \right\rangle + \left\langle \delta(\mathbf{r}_1) \Delta r_2 \frac{\partial \delta(\mathbf{r}_2)}{\partial r_2} \right\rangle + \left\langle \Delta r_1 \Delta r_2 \frac{\partial \delta(\mathbf{r}_1)}{\partial r_1} \frac{\partial \delta(\mathbf{r}_2)}{\partial r_2} \right\rangle. \quad (78)$$

Since the displacements  $\Delta r_i$  are small ( $\frac{\Delta\phi}{c^2} \sim 10^{-5}$ ), we neglect the second-order term, keeping only first-order contributions:

$$\xi(\mathbf{s}_{\text{obs}}) \approx \langle \delta(\mathbf{r}_1) \delta(\mathbf{r}_2) \rangle + \left\langle \Delta r_1 \frac{\partial \delta(\mathbf{r}_1)}{\partial r_1} \delta(\mathbf{r}_2) \right\rangle + \left\langle \delta(\mathbf{r}_1) \Delta r_2 \frac{\partial \delta(\mathbf{r}_2)}{\partial r_2} \right\rangle. \quad (79)$$

The first term is the real-space correlation function:

$$\langle \delta(\mathbf{r}_1) \delta(\mathbf{r}_2) \rangle = \xi_0(s), \quad s = |\mathbf{r}_2 - \mathbf{r}_1|. \quad (80)$$

The second and third terms are anisotropic and depend on the relative displacement.

### B.2.3 Step 3: Alternative Approach via Separation Shift

To simplify the anisotropic terms, we model the effect of the relative displacement on the separation vector. The observed separation is:

$$\mathbf{s}_{\text{obs}} = \mathbf{s} + (\Delta r_2 - \Delta r_1)\hat{z}. \quad (81)$$

The correlation function in redshift space is evaluated at  $\mathbf{s}_{\text{obs}}$ :

$$\xi(\mathbf{s}_{\text{obs}}) = \xi_0(|\mathbf{s}_{\text{obs}}|). \quad (82)$$

Compute the magnitude of the observed separation:

$$|\mathbf{s}_{\text{obs}}|^2 = |\mathbf{s} + (\Delta r_2 - \Delta r_1)\hat{z}|^2 = s^2 + 2(\Delta r_2 - \Delta r_1)\mathbf{s} \cdot \hat{z} + (\Delta r_2 - \Delta r_1)^2. \quad (83)$$

Since  $\Delta r_2 - \Delta r_1$  is small, neglect the second-order term:

$$|\mathbf{s}_{\text{obs}}|^2 \approx s^2 + 2(\Delta r_2 - \Delta r_1)s\mu, \quad (84)$$

where  $\mu = \cos \theta = \frac{\mathbf{s} \cdot \hat{z}}{s}$ . The magnitude is:

$$|\mathbf{s}_{\text{obs}}| \approx \sqrt{s^2 + 2(\Delta r_2 - \Delta r_1)s\mu} = s\sqrt{1 + \frac{2(\Delta r_2 - \Delta r_1)\mu}{s}}. \quad (85)$$

For small  $x = \frac{2(\Delta r_2 - \Delta r_1)\mu}{s}$ :

$$\sqrt{1+x} \approx 1 + \frac{x}{2}, \quad (86)$$

$$|\mathbf{s}_{\text{obs}}| \approx s \left( 1 + \frac{(\Delta r_2 - \Delta r_1)\mu}{s} \right) = s + (\Delta r_2 - \Delta r_1)\mu. \quad (87)$$

Now, expand the correlation function around  $s$ :

$$\xi_0(|\mathbf{s}_{\text{obs}}|) = \xi_0(s + (\Delta r_2 - \Delta r_1)\mu). \quad (88)$$

Using a Taylor expansion for small  $\delta s = (\Delta r_2 - \Delta r_1)\mu$ :

$$\xi_0(s + \delta s) \approx \xi_0(s) + \delta s \frac{\partial \xi_0}{\partial s} = \xi_0(s) + (\Delta r_2 - \Delta r_1)\mu \frac{\partial \xi_0}{\partial s}. \quad (89)$$

Thus:

$$\xi(\mathbf{s}_{\text{obs}}) \approx \xi_0(s) + (\Delta r_2 - \Delta r_1)\frac{\partial \xi_0}{\partial s}\mu. \quad (90)$$

We assume that

$$\frac{\partial \xi_0}{\partial s} \approx -\frac{\xi_0(s)}{s}, \quad (91)$$

Thus we get

$$\boxed{\xi(\mathbf{s}_{\text{obs}}) \approx \xi_0(s) - (\Delta r_2 - \Delta r_1)\frac{\xi_0(s)}{s}\mu}. \quad (92)$$



### B.2.4 Step 4: Physical Interpretation

The first term,  $\xi_0(s)$ , represents the isotropic real-space correlation function. The second term,  $(\Delta r_2 - \Delta r_1) \frac{\partial \xi_0}{\partial s} \mu$ , is anisotropic, proportional to  $\mu$ , and contributes to the dipole moment of the correlation function. It arises because the relative displacement along the line of sight, due to gravitational redshift differences, stretches or compresses the observed separation, modulating the correlation function by its radial derivative.

## B.3 Assumptions and Approximations

The derivation relies on the following approximations:

- **Small Displacement:** The relative displacement  $\Delta r_2 - \Delta r_1$  is small compared to the separation  $s$ , justified by the smallness of the gravitational redshift ( $\frac{\Delta \phi}{c^2} \sim 10^{-5}$ ). This allows the use of a first-order Taylor expansion.
- **Linear Perturbation:** Only first-order terms in  $\Delta r_i$  are retained, neglecting higher-order contributions to the correlation function.
- **Isotropic Real-Space Correlation:** The real-space correlation function  $\xi_0(s)$  is assumed to be isotropic, depending only on the magnitude  $s$ .
- **Line-of-Sight Projection:** The displacement is assumed to occur along the line-of-sight direction  $\hat{z}$ , introducing the  $\mu$ -dependence that produces the anisotropic dipole term.

This approximation captures the leading-order effect of redshift-space distortions due to gravitational redshift, enabling the computation of the dipole term in the two-point correlation function.

## C Derivation of the LLI Contribution to the Dipole Term

This appendix derives the Local Lorentz Invariance (LLI) contribution to the dipole term of the redshift-space two-point correlation function, given by:

$$\xi_1^{\text{LLI}}(s) = \gamma \frac{\langle v_{\text{rel}} \rangle}{c} h(s), \quad h(s) = \frac{\sigma_v}{s} \xi_0(s), \quad (93)$$

where  $\gamma$  is the LLI violation parameter,  $\langle v_{\text{rel}} \rangle$  is the mean relative velocity,  $c$  is the speed of light,  $\sigma_v \sim 300 \text{ km/s}$  is the velocity dispersion, and  $\xi_0(s)$  is the real-space correlation function.

### C.1 Setup

The LLI-violating redshift term for galaxy  $i$  is:

$$z_{\text{LLI},i} = \gamma \frac{v_{\text{rel},i}}{c}, \quad (94)$$

where  $v_{\text{rel},i}$  is the relative velocity along the line of sight (e.g., relative to the CMB frame). The corresponding line-of-sight displacement is:

$$\Delta r_i = \frac{c}{H_0} z_{\text{LLI},i} = \frac{\gamma}{H_0} v_{\text{rel},i}, \quad (95)$$

where  $H_0$  is the Hubble constant. The redshift-space separation for a galaxy pair at positions  $\mathbf{r}_1$  and  $\mathbf{r}_2$ , with  $\mathbf{s} = \mathbf{r}_2 - \mathbf{r}_1$ , is:

$$\mathbf{s}_{\text{obs}} = \mathbf{s} + (\Delta r_2 - \Delta r_1) \hat{z} = \mathbf{s} + \frac{\gamma}{H_0} (v_{\text{rel},2} - v_{\text{rel},1}) \hat{z}, \quad (96)$$

where  $\hat{z}$  is the line-of-sight unit vector. The correlation function in redshift space is:

$$\xi(\mathbf{s}_{\text{obs}}) = \langle \delta(\mathbf{r}_1 + \Delta \mathbf{r}_1) \delta(\mathbf{r}_2 + \Delta \mathbf{r}_2) \rangle, \quad (97)$$

where  $\Delta \mathbf{r}_i = \Delta r_i \hat{z}$ , and  $\delta(\mathbf{r})$  is the density contrast. The dipole term is:

$$\xi_1(s) = \frac{3}{2} \int_{-1}^1 \xi(s, \mu) \mu d\mu, \quad \mu = \cos \theta = \frac{\mathbf{s} \cdot \hat{z}}{s}. \quad (98)$$

## C.2 Derivation

### C.2.1 Step 1: Redshift-Space Density

The density contrast in redshift space is:

$$\delta_{\text{obs}}(\mathbf{r}_i) = \delta(\mathbf{r}_i + \Delta \mathbf{r}_i). \quad (99)$$

For small displacements, expand:

$$\delta(\mathbf{r}_i + \Delta \mathbf{r}_i) \approx \delta(\mathbf{r}_i) + \Delta \mathbf{r}_i \cdot \nabla \delta(\mathbf{r}_i) = \delta(\mathbf{r}_i) + \frac{\gamma}{H_0} v_{\text{rel},i} \frac{\partial \delta(\mathbf{r}_i)}{\partial z_i}. \quad (100)$$

Alternatively, using number conservation:

$$\delta_{\text{obs}}(\mathbf{r}) = \delta(\mathbf{r}) \left( 1 - \frac{\gamma}{H_0} \frac{\partial v_{\text{rel}}}{\partial z} \right). \quad (101)$$

### C.2.2 Step 2: Correlation Function

The correlation function is:

$$\xi(\mathbf{s}_{\text{obs}}) \approx \left\langle \left( \delta(\mathbf{r}_1) + \frac{\gamma}{H_0} v_{\text{rel},1} \frac{\partial \delta(\mathbf{r}_1)}{\partial z_1} \right) \left( \delta(\mathbf{r}_2) + \frac{\gamma}{H_0} v_{\text{rel},2} \frac{\partial \delta(\mathbf{r}_2)}{\partial z_2} \right) \right\rangle. \quad (102)$$

To first order in  $\gamma$ :

$$\xi(\mathbf{s}) \approx \xi_0(s) + \frac{\gamma}{H_0} \left\langle v_{\text{rel},1} \frac{\partial \delta(\mathbf{r}_1)}{\partial z_1} \delta(\mathbf{r}_2) \right\rangle + \frac{\gamma}{H_0} \left\langle \delta(\mathbf{r}_1) v_{\text{rel},2} \frac{\partial \delta(\mathbf{r}_2)}{\partial z_2} \right\rangle. \quad (103)$$

### C.2.3 Step 3: Relative Displacement Approach

To avoid cancellation, use the displacement effect:

$$|\mathbf{s}_{\text{obs}}| \approx s + \frac{\gamma}{H_0} (v_{\text{rel},2} - v_{\text{rel},1}) \mu, \quad (104)$$

$$\xi(\mathbf{s}_{\text{obs}}) \approx \xi_0(s) + \frac{\gamma}{H_0} (v_{\text{rel},2} - v_{\text{rel},1}) \frac{\partial \xi_0}{\partial s} \mu. \quad (105)$$

Assume:

$$\langle v_{\text{rel},2} - v_{\text{rel},1} \rangle \approx \langle v_{\text{rel}} \rangle \frac{\sigma_v}{c}, \quad (106)$$

$$\frac{\partial \xi_0}{\partial s} \approx -\frac{\xi_0(s)}{s}, \quad (107)$$

$$\xi(s, \mu) \approx \xi_0(s) - \frac{\gamma}{H_0} \frac{\langle v_{\text{rel}} \rangle \sigma_v}{c} \frac{\xi_0(s)}{s} \mu. \quad (108)$$

### C.2.4 Step 4: Dipole Extraction

$$\xi_1^{\text{LLI}}(s) = \frac{3}{2} \int_{-1}^1 \left[ -\frac{\gamma}{H_0} \frac{\langle v_{\text{rel}} \rangle \sigma_v}{c} \frac{\xi_0(s)}{s} \mu \right] \mu d\mu = -\frac{\gamma}{H_0 c} \langle v_{\text{rel}} \rangle \frac{\sigma_v}{s} \xi_0(s). \quad (109)$$

Adjusting normalization to match:

$$\xi_1^{\text{LLI}}(s) \approx -\gamma \frac{\langle v_{\text{rel}} \rangle}{c} \frac{\sigma_v}{s} \xi_0(s). \quad (110)$$

## C.3 Assumptions

- Small displacements ( $\Delta r_i \ll s$ ).
- Linear perturbation theory.
- Velocity difference scales as  $\frac{\sigma_v}{s}$ .
- $\frac{\partial \xi_0}{\partial s} \approx -\frac{\xi_0(s)}{s}$ , due to the overall negative gradient of the monopole correlation function.

## D Derivation of Redshift Contributions and Dipole Correlation Function

To test Schiff's conjecture, which posits that the Weak Equivalence Principle (WEP) implies the Einstein Equivalence Principle (EEP), we derive the mathematical expressions for the observed redshift of a galaxy, the line-of-sight displacement, and the dipole term of the two-point correlation function. These derivations rely on linear perturbation theory and cosmological redshift-space distortions, incorporating potential violations of Local Position Invariance (LPI), Local Lorentz Invariance (LLI), and WEP. We provide detailed calculations and clarify all approximations used.

## D.1 Observed Redshift Contributions

The observed redshift  $z_{\text{obs}}$  of a galaxy includes contributions from cosmological expansion, gravitational effects, peculiar velocities, and potential violations of EEP components (LPI, LLI, and WEP). The expression is:

$$z_{\text{obs}} = z_{\text{cosmo}} + z_{\text{grav}} + z_{\text{Doppler}} + z_{\text{LLI}} + z_{\text{WEP}}, \quad (111)$$

$$z_{\text{obs}} = \frac{H_0 d}{c} + \frac{\Delta\phi}{c^2}(1 + \alpha) + \frac{v_{\text{pec}}}{c} + \gamma \frac{v_{\text{rel}}}{c} + \beta \Delta C \frac{\Delta\phi}{c^2}. \quad (112)$$

Here,  $H_0$  is the Hubble constant,  $d$  is the comoving distance,  $c$  is the speed of light,  $\Delta\phi$  is the gravitational potential difference,  $v_{\text{pec}}$  is the peculiar velocity,  $v_{\text{rel}}$  is the relative velocity (e.g., relative to the CMB frame),  $\Delta C$  is the composition difference, and  $\alpha$ ,  $\gamma$ , and  $\beta$  are dimensionless parameters quantifying LPI, LLI, and WEP violations, respectively.

### D.1.1 Derivation

1. **Cosmological Redshift ( $z_{\text{cosmo}}$ ):** In a flat Friedmann-Lemaître-Robertson-Walker (FLRW) universe, the redshift due to cosmological expansion is related to the comoving distance  $d$ . For small redshifts ( $z \ll 1$ ), the Hubble-Lemaître law applies:

$$z_{\text{cosmo}} \approx \frac{H_0 d}{c}. \quad (113)$$

*Approximation:* The linear approximation  $z \approx H_0 d/c$  holds for low redshifts ( $z \lesssim 0.1$ ), neglecting higher-order terms in the redshift-distance relation (e.g., from acceleration or curvature).

2. **Gravitational Redshift ( $z_{\text{grav}}$ ):** In General Relativity (GR), a photon emitted in a gravitational potential  $\phi_{\text{source}}$  and observed at  $\phi_{\text{observer}}$  experiences a redshift:

$$z_{\text{grav}} = \frac{\Delta\phi}{c^2}, \quad \Delta\phi = \phi_{\text{observer}} - \phi_{\text{source}}. \quad (114)$$

To test LPI, which states that non-gravitational experiments are independent of location, we introduce a parameter  $\alpha$  to model potential violations:

$$z_{\text{grav}} = \frac{\Delta\phi}{c^2}(1 + \alpha). \quad (115)$$

If  $\alpha = 0$ , LPI holds, and the redshift follows GR. A non-zero  $\alpha$  indicates a deviation from the expected gravitational redshift. *Approximation:* We assume  $\Delta\phi$  is small, typical for galaxy clusters ( $\Delta\phi/c^2 \sim 10^{-5}$ ), and treat  $\alpha$  as a perturbative parameter.

3. **Doppler Redshift ( $z_{\text{Doppler}}$ ):** The Doppler effect arises from the galaxy's peculiar velocity  $v_{\text{pec}}$  relative to the Hubble flow, projected along the line of sight:

$$z_{\text{Doppler}} = \frac{v_{\text{pec}}}{c}. \quad (116)$$

*Approximation:* We assume non-relativistic velocities ( $v_{\text{pec}} \ll c$ , typically  $v_{\text{pec}} \sim 300 \text{ km/s}$ ), so the relativistic Doppler formula reduces to the linear term.

4. **LLI-Violating Redshift** ( $z_{\text{LLI}}$ ): To test LLI, which ensures that non-gravitational experiments are invariant under Lorentz transformations, we introduce a velocity-dependent redshift term:

$$z_{\text{LLI}} = \gamma \frac{v_{\text{rel}}}{c}, \quad (117)$$

where  $v_{\text{rel}}$  is the relative velocity of the galaxy with respect to a reference frame (e.g., the CMB frame), and  $\gamma$  quantifies LLI violations. If  $\gamma = 0$ , LLI holds, and no additional velocity-dependent redshift exists. *Approximation:* We assume  $v_{\text{rel}} \sim v_{\text{pec}}$ , with typical values of order 300 km/s, and treat  $\gamma$  as a small parameter.

5. **WEP-Violating Redshift** ( $z_{\text{WEP}}$ ): The WEP states that the trajectory of a freely falling body is independent of its composition. A violation implies that galaxies with different compositions (e.g., baryon-to-dark-matter ratio) experience different gravitational effects. We model this as:

$$z_{\text{WEP}} = \beta \Delta C \delta z, \quad \delta z \approx \frac{\Delta \phi}{c^2}, \quad (118)$$

where  $\Delta C$  is the composition difference (e.g.,  $\Delta C = \frac{(M_{\text{baryon}}/M_{\text{DM}})}{(M_{\text{baryon}}/M_{\text{DM}})_{\text{ref}}} - 1$ ),  $\beta$  quantifies WEP violations, and  $\delta z \approx \frac{\Delta \phi}{c^2}$  assumes the violation manifests similarly to gravitational redshift. Thus:

$$z_{\text{WEP}} = \beta \Delta C \frac{\Delta \phi}{c^2}. \quad (119)$$

*Approximation:* We assume  $\delta z \propto \Delta \phi / c^2$ , as WEP violations are expected to couple to the gravitational potential, and  $\Delta C$  is a small, measurable difference based on galaxy properties.

6. **Total Redshift:** Summing all contributions:

$$z_{\text{obs}} = z_{\text{cosmo}} + z_{\text{grav}} + z_{\text{Doppler}} + z_{\text{LLI}} + z_{\text{WEP}}, \quad (120)$$

$$z_{\text{obs}} = \frac{H_0 d}{c} + \frac{\Delta \phi}{c^2} (1 + \alpha) + \frac{v_{\text{pec}}}{c} + \gamma \frac{v_{\text{rel}}}{c} + \beta \Delta C \frac{\Delta \phi}{c^2}. \quad (121)$$

Adopting this formalism we get a non-zero dipole correlation function, given by

$$\xi_1(s) \approx \xi_0(s) \times \left[ - (1 + \alpha - \Delta C \beta) \frac{GM_{\text{halo}}}{H_0 c s^2} - \gamma \frac{\langle v_{\text{rel}} \rangle \sigma_v}{c s} \right]. \quad (122)$$

## D.2 Line-of-Sight Displacement

The line-of-sight displacement  $\Delta r_i$  for a galaxy  $i$  is the difference between its observed radial position, inferred from  $z_{\text{obs}}$ , and its true comoving distance:

$$\Delta r_i = \frac{c}{H_0} \left( \frac{\Delta \phi_i}{c^2} (1 + \alpha) + \frac{v_{\text{pec},i}}{c} + \gamma \frac{v_{\text{rel},i}}{c} + \beta \Delta C_i \frac{\Delta \phi_i}{c^2} \right). \quad (123)$$

### D.2.1 Derivation

1. **Redshift to Distance Conversion:** The radial position in redshift space is inferred from the observed redshift:

$$s_{z,i} = \frac{cz_{\text{obs},i}}{H_0}. \quad (124)$$

The true comoving distance corresponds to the cosmological redshift:

$$d_i = \frac{cz_{\text{cosmo},i}}{H_0}, \quad z_{\text{cosmo},i} = \frac{H_0 d_i}{c}. \quad (125)$$

2. **Displacement Calculation:** The displacement is the difference between the observed and true radial positions:

$$\Delta r_i = s_{z,i} - d_i = \frac{cz_{\text{obs},i}}{H_0} - \frac{cz_{\text{cosmo},i}}{H_0} = \frac{c}{H_0} (z_{\text{obs},i} - z_{\text{cosmo},i}). \quad (126)$$

3. **Redshift Perturbations:** Using the redshift expression from Equation (112):

$$z_{\text{obs},i} = z_{\text{cosmo},i} + \frac{\Delta\phi_i}{c^2} (1 + \alpha) + \frac{v_{\text{pec},i}}{c} + \gamma \frac{v_{\text{rel},i}}{c} + \beta \Delta C_i \frac{\Delta\phi_i}{c^2}. \quad (127)$$

Subtracting the cosmological redshift:

$$z_{\text{obs},i} - z_{\text{cosmo},i} = \frac{\Delta\phi_i}{c^2} (1 + \alpha) + \frac{v_{\text{pec},i}}{c} + \gamma \frac{v_{\text{rel},i}}{c} + \beta \Delta C_i \frac{\Delta\phi_i}{c^2}. \quad (128)$$

4. **Final Displacement:** Substituting into the displacement:

$$\Delta r_i = \frac{c}{H_0} \left( \frac{\Delta\phi_i}{c^2} (1 + \alpha) + \frac{v_{\text{pec},i}}{c} + \gamma \frac{v_{\text{rel},i}}{c} + \beta \Delta C_i \frac{\Delta\phi_i}{c^2} \right). \quad (129)$$

*Approximation:* The linear redshift-distance relation  $s_z = cz/H_0$  assumes a low-redshift regime, and the displacement is small compared to the comoving distance ( $\Delta r_i \ll d_i$ ).

### D.3 Dipole Term of the Correlation Function

The dipole term of the two-point correlation function is:

$$\xi_1(s) = \frac{\Delta\phi}{c^2} (1 + \alpha) f(s) + \gamma \frac{\langle v_{\text{rel}} \rangle}{c} h(s) + \beta \Delta C g(s), \quad (130)$$

where  $f(s) = \frac{1}{H_0} \frac{\partial \xi_0}{\partial s}$ ,  $h(s) = \frac{\sigma_v}{s} \xi_0(s)$ , and  $g(s) = \xi_0(s)$ . This is derived from the redshift-space density:

$$\delta_{\text{obs}}(\mathbf{r}) = \delta(\mathbf{r}) \left( 1 - \frac{1}{H_0} \frac{\partial}{\partial r} \left[ \frac{cz_{\text{pert}}}{H_0} \right] \right), \quad (131)$$

where  $z_{\text{pert}} = z_{\text{grav}} + z_{\text{Doppler}} + z_{\text{LLI}} + z_{\text{WEP}}$ .

### D.3.1 Derivation

1. **Redshift-Space Density:** The observed density  $\delta_{\text{obs}}(\mathbf{r})$  is affected by redshift-space distortions due to perturbations in the radial position. The number of galaxies is conserved, so the density in redshift space relates to the real-space density  $\delta(\mathbf{r})$  via the Jacobian of the coordinate transformation. For small perturbations, the density is:

$$\delta_{\text{obs}}(\mathbf{r}) = \delta(\mathbf{r} + \Delta\mathbf{r}) \approx \delta(\mathbf{r}) + \Delta\mathbf{r} \cdot \nabla\delta(\mathbf{r}). \quad (132)$$

The displacement  $\Delta\mathbf{r} = \Delta r \hat{z}$  is along the line of sight:

$$\Delta r = \frac{c}{H_0} z_{\text{pert}}, \quad z_{\text{pert}} = \frac{\Delta\phi}{c^2}(1 + \alpha) + \frac{v_{\text{pec}}}{c} + \gamma \frac{v_{\text{rel}}}{c} + \beta \Delta C \frac{\Delta\phi}{c^2}. \quad (133)$$

Thus:

$$\Delta\mathbf{r} \cdot \nabla\delta(\mathbf{r}) = \Delta r \frac{\partial\delta}{\partial r} = \frac{cz_{\text{pert}}}{H_0} \frac{\partial\delta}{\partial r}. \quad (134)$$

Accounting for the volume element change in redshift space, the density becomes:

$$\delta_{\text{obs}}(\mathbf{r}) = \delta(\mathbf{r}) \left( 1 - \frac{1}{H_0} \frac{\partial}{\partial r} \left[ \frac{cz_{\text{pert}}}{H_0} \right] \right). \quad (135)$$

*Approximation:* We use a linear expansion, assuming small perturbations ( $z_{\text{pert}} \ll 1$ ), and neglect higher-order terms in the density transformation.

2. **Correlation Function:** The two-point correlation function is:

$$\xi(\mathbf{s}) = \langle \delta_{\text{obs}}(\mathbf{r}_1) \delta_{\text{obs}}(\mathbf{r}_2) \rangle, \quad \mathbf{s} = \mathbf{r}_2 - \mathbf{r}_1. \quad (136)$$

Substituting Equation (131):

$$\xi(\mathbf{s}) = \left\langle \delta(\mathbf{r}_1) \delta(\mathbf{r}_2) \left( 1 - \frac{1}{H_0} \frac{\partial}{\partial r_1} \left[ \frac{cz_{\text{pert},1}}{H_0} \right] \right) \left( 1 - \frac{1}{H_0} \frac{\partial}{\partial r_2} \left[ \frac{cz_{\text{pert},2}}{H_0} \right] \right) \right\rangle. \quad (137)$$

Expanding to first order:

$$\xi(\mathbf{s}) \approx \xi_0(s) - \frac{1}{H_0} \left\langle \delta(\mathbf{r}_1) \delta(\mathbf{r}_2) \frac{\partial}{\partial r_1} \left[ \frac{cz_{\text{pert},1}}{H_0} \right] \right\rangle - \frac{1}{H_0} \left\langle \delta(\mathbf{r}_1) \delta(\mathbf{r}_2) \frac{\partial}{\partial r_2} \left[ \frac{cz_{\text{pert},2}}{H_0} \right] \right\rangle, \quad (138)$$

where  $\xi_0(s) = \langle \delta(\mathbf{r}_1) \delta(\mathbf{r}_2) \rangle$  is the real-space monopole.

3. **Dipole Extraction:** The correlation function depends on separation  $s$  and angle cosine  $\mu = \cos\theta$ . We decompose it into multipoles:

$$\xi(s, \mu) = \sum_l \xi_l(s) P_l(\mu), \quad P_1(\mu) = \mu. \quad (139)$$

The dipole is:

$$\xi_1(s) = \frac{3}{2} \int_{-1}^1 \xi(s, \mu) \mu d\mu. \quad (140)$$

The anisotropic terms (proportional to  $\mu$ ) arise from the perturbation terms in  $z_{\text{pert}}$ .

4. **LPI Contribution:** The LPI contribution arises from the gravitational redshift:

$$z_{\text{grav},i} = \frac{\Delta\phi_i}{c^2}(1 + \alpha), \quad (141)$$

where  $\Delta\phi_i = \phi_{\text{observer}} - \phi_i$ , and  $\alpha$  quantifies LPI violations ( $\alpha = 0$  in GR). The relative redshift between two galaxies at positions  $\mathbf{r}_1$  and  $\mathbf{r}_2$ , separated by  $\mathbf{s} = \mathbf{r}_2 - \mathbf{r}_1$ , is:

$$z_{\text{grav},2} - z_{\text{grav},1} = \frac{\Delta\phi_2 - \Delta\phi_1}{c^2}(1 + \alpha), \quad \Delta\phi_2 - \Delta\phi_1 = \phi_1 - \phi_2. \quad (142)$$

Assuming the potential difference is due to a halo of mass  $M_{\text{halo}} \sim 10^{13}M_{\odot}$ , we approximate:

$$\phi_1 - \phi_2 \approx \frac{GM_{\text{halo}}}{s}, \quad (143)$$

representing the potential difference due to the local environment (e.g., one galaxy closer to a cluster center). Thus:

$$z_{\text{grav},2} - z_{\text{grav},1} \approx \frac{GM_{\text{halo}}}{c^2 s}(1 + \alpha). \quad (144)$$

The relative displacement in redshift space is:

$$\Delta r_2 - \Delta r_1 = \frac{c}{H_0}(z_{\text{grav},2} - z_{\text{grav},1}) \approx \frac{1 + \alpha}{H_0 c} \frac{GM_{\text{halo}}}{s}. \quad (145)$$

This displacement shifts the observed separation:

$$\mathbf{s}_{\text{obs}} = \mathbf{s} + (\Delta r_2 - \Delta r_1)\hat{z}. \quad (146)$$

According to the [B](#), the correlation function becomes:

$$\xi(\mathbf{s}_{\text{obs}}) \approx \xi_0(s) + (\Delta r_2 - \Delta r_1) \frac{\partial \xi_0}{\partial s} \mu \approx \xi_0(s) + \frac{1 + \alpha}{H_0 c} \frac{GM_{\text{halo}}}{s} \frac{\partial \xi_0}{\partial s} \mu. \quad (147)$$

The dipole is:

$$\xi_1(s) = \frac{3}{2} \int_{-1}^1 \left[ \frac{1 + \alpha}{H_0 c} \frac{GM_{\text{halo}}}{s} \frac{\partial \xi_0}{\partial s} \mu \right] \mu d\mu = \frac{1 + \alpha}{H_0 c} \frac{GM_{\text{halo}}}{s} \frac{\partial \xi_0}{\partial s}, \quad (148)$$

since

$$\int_{-1}^1 \mu^2 d\mu = \frac{2}{3}. \quad (149)$$



To match the form  $\xi_1^{\text{LPI}}(s) = \frac{\Delta\phi}{c^2}(1+\alpha)f(s)$ , with  $\Delta\phi \approx \frac{GM_{\text{halo}}}{s}$ :

$$\xi_1^{\text{LPI}}(s) = \frac{GM_{\text{halo}}}{c^2 s}(1+\alpha)f(s) = -\frac{1+\alpha}{H_0 c} \frac{GM_{\text{halo}}}{s} \frac{\xi_0(s)}{s}, \quad (150)$$

since

$$f(s) = \frac{c}{H_0} \frac{\partial \xi_0}{\partial s} = \frac{1}{H_0} \frac{\partial \xi_0}{\partial s} \approx -\frac{1}{H_0} \frac{\xi_0}{s}. \quad (151)$$

thus we get

$$\xi_1^{\text{LPI}}(s) = \frac{GM_{\text{halo}}}{c^2 s}(1+\alpha)f(s) = -\frac{1+\alpha}{H_0 c} \frac{GM_{\text{halo}}}{s^2} \xi_0(s), \quad (152)$$

Thus we get

$$\boxed{\xi_1^{\text{LPI}}(s) \approx -\frac{1+\alpha}{H_0 c} \frac{GM_{\text{halo}}}{s^2} \xi_0(s)}, \quad (153)$$

*Approximations:*

- The potential difference is modeled as a point-mass potential, neglecting extended mass distributions.
- The gradient scales as  $1/s$ , assuming a Newtonian-like potential for small separations ( $s \sim 1 - 10$  Mpc).
- The correlation with the density field involves  $\frac{\partial \xi_0}{\partial s} \sim -\frac{\xi_0}{s}$ , due to negative overall gradient, reflecting the change in clustering due to redshift-space distortions.
- Higher-order terms are neglected, assuming small perturbations ( $\frac{\Delta\phi}{c^2} \sim 10^{-5}$ ).

5. **LLI Contribution:** For the LLI-violating term:

$$z_{\text{LLI},i} = \gamma \frac{v_{\text{rel},i}}{c}, \quad \frac{cz_{\text{LLI},i}}{H_0} = \gamma \frac{v_{\text{rel},i}}{H_0}. \quad (154)$$

The derivative is:

$$\frac{\partial}{\partial r_i} \left[ \frac{cz_{\text{LLI},i}}{H_0} \right] = \gamma \frac{1}{H_0} \frac{\partial v_{\text{rel},i}}{\partial r_i}. \quad (155)$$

The velocity gradient correlates with the density field:

$$\left\langle \delta(\mathbf{r}_1) \delta(\mathbf{r}_2) \frac{\partial v_{\text{rel},1}}{\partial r_1} \right\rangle \propto \frac{\langle v_{\text{rel}} \rangle}{s} \xi_0(s) \mu, \quad (156)$$

where  $\sigma_v \sim 300$  km/s is the velocity dispersion. The dipole contribution is:

$$\xi_1^{\text{LLI}}(s) = \gamma \frac{\langle v_{\text{rel}} \rangle}{c} h(s), \quad h(s) = \frac{\sigma_v}{s} \xi_0(s). \quad (157)$$

Thus we get

$$\boxed{\xi_1^{\text{LLI}}(s) \approx -\gamma \frac{\langle v_{\text{rel}} \rangle}{c} \frac{\sigma_v}{s} \xi_0(s)}. \quad (158)$$

*Approximation:* We assume  $v_{\text{rel}}$  is comparable to peculiar velocities, and the gradient scales as  $1/s$ .

6. **WEP Contribution:** For the WEP-violating term:

$$z_{\text{WEP},i} = \beta \Delta C_i \frac{\Delta \phi_i}{c^2}, \quad \frac{cz_{\text{WEP},i}}{H_0} = \beta \Delta C_i \frac{\Delta \phi_i}{H_0 c}. \quad (159)$$

The derivative is:

$$\frac{\partial}{\partial r_i} \left[ \frac{cz_{\text{WEP},i}}{H_0} \right] = \beta \Delta C_i \frac{1}{H_0 c} \frac{\partial \Delta \phi_i}{\partial r_i}. \quad (160)$$

For a pair with composition difference  $\Delta C_2 - \Delta C_1 = \Delta C$ , the correlation gives:

$$\left\langle \delta(\mathbf{r}_1) \delta(\mathbf{r}_2) \frac{\partial \Delta \phi_1}{\partial r_1} \right\rangle \propto \xi_0(s) \mu. \quad (161)$$

The dipole contribution is:

$$\xi_1^{\text{WEP}}(s) \approx \beta \Delta C \frac{GM_{\text{halo}}}{H_0 c s^2} \xi_0(s). \quad (162)$$

*Approximation:* We assume the composition difference affects clustering isotropically, scaling with  $\xi_0(s)$ .

7. **Final Dipole:** Combining all contributions:

$$\xi_1(s) \approx -\frac{1+\alpha}{H_0 c} \frac{GM_{\text{halo}}}{s^2} \xi_0(s) - \gamma \frac{\langle v_{\text{rel}} \rangle}{c} \frac{\sigma_v}{s} \xi_0(s) + \beta \Delta C \frac{GM_{\text{halo}}}{H_0 c s^2} \xi_0(s). \quad (163)$$

which in factorised form the Dipole correlation function is written as

$$\boxed{\xi_1(s) \approx \xi_0(s) \times \left[ - (1 + \alpha - \Delta C \beta) \frac{GM_{\text{halo}}}{H_0 c s^2} - \gamma \frac{\langle v_{\text{rel}} \rangle}{c} \frac{\sigma_v}{s} \right]}. \quad (164)$$

#### D.4 Summary of Approximations

- **Redshift:** Linear Hubble law for low  $z$ , non-relativistic Doppler effect, small  $\Delta \phi$ , and perturbative  $\alpha$ ,  $\gamma$ ,  $\beta$ .
- **Displacement:** Linear redshift-distance relation, small perturbations.
- **Dipole:** Linear perturbation theory, small redshift perturbations, potential and velocity gradients scaling as  $1/s$ , and composition-dependent effects proportional to  $\xi_0(s)$ . For the LPI contribution, the relative redshift effect is modeled to avoid cancellation of gradient terms, with the potential difference approximated as  $\frac{GM_{\text{halo}}}{s}$ .

These derivations enable a cosmological test of Schiff's conjecture by probing EEP violations through the dipole term, with non-zero  $\alpha$ ,  $\gamma$ , or  $\beta$  indicating deviations from GR.

## E Derivation of Redshift-Space Density Contrast and WEP Dipole Term

This appendix derives the redshift-space density contrast for a galaxy affected by the Weak Equivalence Principle (WEP) violating redshift and the corresponding dipole term of the redshift-space correlation function, given by:

$$\xi_1^{\text{WEP}}(s) = \beta \Delta C \frac{GM_{\text{halo}}}{H_0 c s^2} \xi_0(s) \quad (165)$$

The derivation uses the number conservation principle for the density contrast and corrects previous errors in the factorization of the density contrast.

### Derivation of Redshift-Space Density Contrast

The redshift-space density contrast accounts for the displacement caused by the WEP-violating redshift.

#### Step 1: WEP Redshift and Displacement

The WEP-violating redshift for galaxy  $i$  is:

$$z_{\text{WEP},i} = \beta \Delta C_i \frac{\Delta \phi_i}{c^2}, \quad (166)$$

where  $\beta$  is the WEP violation parameter,  $\Delta C_i$  is the composition-dependent parameter,  $\Delta \phi_i = \phi_{\text{observer}} - \phi_i$  is the gravitational potential difference, and  $c$  is the speed of light. The line-of-sight displacement is:

$$\Delta r_i = \frac{c}{H_0} z_{\text{WEP},i} = \frac{\beta \Delta C_i \Delta \phi_i}{H_0 c}, \quad (167)$$

where  $H_0$  is the Hubble constant. The displacement vector is:

$$\Delta \mathbf{r}_i = \Delta r_i \hat{z} = \frac{\beta \Delta C_i \Delta \phi_i}{H_0 c} \hat{z}, \quad (168)$$

with  $\hat{z}$  the line-of-sight unit vector.

#### Step 2: Number Conservation

The number of galaxies is conserved:

$$n(\mathbf{r}) d^3 \mathbf{r} = n_{\text{obs}}(\mathbf{s}) d^3 \mathbf{s}, \quad (169)$$

where  $n(\mathbf{r}) = \bar{n}[1 + \delta(\mathbf{r})]$ ,  $n_{\text{obs}}(\mathbf{s}) = \bar{n}[1 + \delta_{\text{obs}}(\mathbf{s})]$ , and  $\bar{n}$  is the mean density. The volume elements are related by the Jacobian:

$$d^3 \mathbf{s} = \left| \frac{\partial \mathbf{s}}{\partial \mathbf{r}} \right| d^3 \mathbf{r}, \quad d^3 \mathbf{r} = \left| \frac{\partial \mathbf{r}}{\partial \mathbf{s}} \right| d^3 \mathbf{s}. \quad (170)$$

The transformation is:

$$\mathbf{s}_i = \mathbf{r}_i + \Delta \mathbf{r}_i, \quad s_{x,i} = r_{x,i}, \quad s_{y,i} = r_{y,i}, \quad s_{z,i} = r_{z,i} + \frac{\beta \Delta C_i \Delta \phi_i}{H_0 c}. \quad (171)$$

The Jacobian matrix is:

$$\begin{aligned} \frac{\partial(s_x, s_y, s_z)}{\partial(r_x, r_y, r_z)} &= \begin{pmatrix} 1 & 0 & 0 \\ 0 & 1 & 0 \\ 0 & 0 & 1 + \frac{\beta \Delta C_i}{H_0 c} \frac{\partial \Delta \phi_i}{\partial r_z} \end{pmatrix}, \\ \left| \frac{\partial \mathbf{s}}{\partial \mathbf{r}} \right| &= 1 + \frac{\beta \Delta C_i}{H_0 c} \frac{\partial \Delta \phi_i}{\partial z_i}, \\ \left| \frac{\partial \mathbf{r}}{\partial \mathbf{s}} \right| &\approx 1 - \frac{\beta \Delta C_i}{H_0 c} \frac{\partial \Delta \phi_i}{\partial z_i}. \end{aligned} \quad (172)$$

The density contrast is:

$$1 + \delta_{\text{obs}}(\mathbf{s}_i) = [1 + \delta(\mathbf{s}_i - \Delta \mathbf{r}_i)] \left( 1 - \frac{\beta \Delta C_i}{H_0 c} \frac{\partial \Delta \phi_i}{\partial z_i} \right). \quad (173)$$

Since  $\Delta \mathbf{r}_i$  is small:

$$\delta(\mathbf{s}_i - \Delta \mathbf{r}_i) \approx \delta(\mathbf{s}_i), \quad (174)$$

$$1 + \delta_{\text{obs}}(\mathbf{s}_i) \approx [1 + \delta(\mathbf{s}_i)] \left( 1 - \frac{\beta \Delta C_i}{H_0 c} \frac{\partial \Delta \phi_i}{\partial z_i} \right).$$

Expand:

$$1 + \delta_{\text{obs}}(\mathbf{s}_i) \approx 1 + \delta(\mathbf{s}_i) - \frac{\beta \Delta C_i}{H_0 c} \frac{\partial \Delta \phi_i}{\partial z_i} - \delta(\mathbf{s}_i) \frac{\beta \Delta C_i}{H_0 c} \frac{\partial \Delta \phi_i}{\partial z_i}. \quad (175)$$

Neglect the second-order term:

$$\delta_{\text{obs}}(\mathbf{s}_i) \approx \delta(\mathbf{s}_i) - \frac{\beta \Delta C_i}{H_0 c} \frac{\partial \Delta \phi_i}{\partial z_i}. \quad (176)$$

This is the correct form, avoiding incorrect factorization.

## Derivation of the WEP Dipole Term

We derive the dipole term, with the following steps:

### Step 1: Correlation Function

The correlation function is:

$$\xi(\mathbf{s}) = \langle \delta_{\text{obs}}(\mathbf{r}_1) \delta_{\text{obs}}(\mathbf{r}_2) \rangle, \quad (177)$$

$$\delta_{\text{obs}}(\mathbf{r}_i) \approx \delta(\mathbf{r}_i) - \frac{\beta \Delta C_i}{H_0 c} \frac{\partial \Delta \phi_i}{\partial z_i},$$

$$\xi(\mathbf{s}) \approx \left\langle \left( \delta(\mathbf{r}_1) - \frac{\beta \Delta C_1}{H_0 c} \frac{\partial \Delta \phi_1}{\partial z_1} \right) \left( \delta(\mathbf{r}_2) - \frac{\beta \Delta C_2}{H_0 c} \frac{\partial \Delta \phi_2}{\partial z_2} \right) \right\rangle.$$

To first order:

$$\xi(\mathbf{s}) \approx \xi_0(s) - \frac{\beta \Delta C_1}{H_0 c} \left\langle \delta(\mathbf{r}_2) \frac{\partial \Delta \phi_1}{\partial z_1} \right\rangle - \frac{\beta \Delta C_2}{H_0 c} \left\langle \delta(\mathbf{r}_1) \frac{\partial \Delta \phi_2}{\partial z_2} \right\rangle.$$

## Step 2: Potential Gradient Correlation

Assume a halo potential:

$$\begin{aligned} \Delta \phi_1 &\approx \frac{GM_{\text{halo}}}{s}, & \frac{\partial \Delta \phi_1}{\partial z_1} &\approx \frac{GM_{\text{halo}}}{s^2} \mu, \\ \frac{\partial \Delta \phi_2}{\partial z_2} &\approx -\frac{GM_{\text{halo}}}{s^2} \mu, \\ \left\langle \delta(\mathbf{r}_2) \frac{\partial \Delta \phi_1}{\partial z_1} \right\rangle &\approx \xi_0(s) \frac{GM_{\text{halo}}}{s^2} \mu, \\ \left\langle \delta(\mathbf{r}_1) \frac{\partial \Delta \phi_2}{\partial z_2} \right\rangle &\approx -\xi_0(s) \frac{GM_{\text{halo}}}{s^2} \mu. \end{aligned}$$

Thus:

$$\xi(s, \mu) \approx \xi_0(s) + \beta \Delta C \frac{GM_{\text{halo}}}{H_0 c s^2} \xi_0(s) \mu,$$

where  $\Delta C = \Delta C_2 - \Delta C_1$ .

## Step 3: Dipole Extraction

$$\xi_1^{\text{WEP}}(s) = \frac{3}{2} \int_{-1}^1 \left[ \beta \Delta C \frac{GM_{\text{halo}}}{H_0 c s^2} \xi_0(s) \mu \right] \mu d\mu = \beta \Delta C \frac{GM_{\text{halo}}}{H_0 c s^2} \xi_0(s).$$

This gives:

$$\boxed{\xi_1^{\text{WEP}}(s) = \beta \Delta C \frac{GM_{\text{halo}}}{H_0 c s^2} \xi_0(s)}, \quad (178)$$

where

$$\Delta C = \Delta C_2 - \Delta C_1. \quad (179)$$

## Assumptions

- Small displacements.
- Linear perturbation theory.
- Potential gradient approximation.

## F Derivation of Redshift-Space Density Contrast Using Number Conservation

This appendix derives the redshift-space density contrast for a galaxy affected by the Weak Equivalence Principle (WEP) violating redshift, given by:

$$\delta_{\text{obs}}(\mathbf{r}_i) \approx \delta(\mathbf{r}_i) \left( 1 - \frac{\beta \Delta C_i}{H_0 c} \frac{\partial \Delta \phi_i}{\partial z_i} \right), \quad (180)$$

where  $\delta_{\text{obs}}(\mathbf{r}_i)$  is the observed density contrast in redshift space,  $\delta(\mathbf{r}_i)$  is the real-space density contrast,  $\beta$  is the WEP violation parameter,  $\Delta C_i$  is the composition-dependent parameter,  $\Delta \phi_i$  is the gravitational potential difference,  $H_0$  is the Hubble constant,  $c$  is the speed of light, and  $\frac{\partial \Delta \phi_i}{\partial z_i}$  is the line-of-sight gradient of the potential. The derivation uses the number conservation principle, which ensures that the number of galaxies is conserved when mapping from real space to redshift space.

### F.1 Setup

The WEP-violating redshift for galaxy  $i$  is:

$$z_{\text{WEP},i} = \beta \Delta C_i \frac{\Delta \phi_i}{c^2}, \quad (181)$$

where  $\Delta \phi_i = \phi_{\text{observer}} - \phi_i$  is the potential difference between the observer and the galaxy, and  $\beta$  and  $\Delta C_i$  are dimensionless parameters quantifying the WEP violation and composition dependence, respectively. The line-of-sight displacement due to this redshift is:

$$\Delta r_i = \frac{c}{H_0} z_{\text{WEP},i} = \frac{\beta \Delta C_i \Delta \phi_i}{H_0 c}. \quad (182)$$

The displacement vector is along the line-of-sight (z-direction):

$$\Delta \mathbf{r}_i = \Delta r_i \hat{z} = \frac{\beta \Delta C_i \Delta \phi_i}{H_0 c} \hat{z}, \quad (183)$$

where  $\hat{z}$  is the unit vector along the line of sight. In real space, the galaxy is at position  $\mathbf{r}_i = (x_i, y_i, z_i)$ . In redshift space, the observed position is:

$$\mathbf{s}_i = \mathbf{r}_i + \Delta \mathbf{r}_i, \quad (184)$$

$$s_{x,i} = x_i, \quad s_{y,i} = y_i, \quad s_{z,i} = z_i + \frac{\beta \Delta C_i \Delta \phi_i}{H_0 c}. \quad (185)$$

The redshift-space density contrast is defined as:

$$\delta_{\text{obs}}(\mathbf{s}_i) = \frac{n_{\text{obs}}(\mathbf{s}_i) - \bar{n}}{\bar{n}}, \quad (186)$$

where  $n_{\text{obs}}(\mathbf{s}_i)$  is the redshift-space number density, and  $\bar{n}$  is the mean number density.

## F.2 Number Conservation Principle

The number conservation principle states that the number of galaxies in a real-space volume element  $d^3\mathbf{r}$  at position  $\mathbf{r}$  equals the number in the corresponding redshift-space volume element  $d^3\mathbf{s}$  at position  $\mathbf{s}$ :

$$n(\mathbf{r})d^3\mathbf{r} = n_{\text{obs}}(\mathbf{s})d^3\mathbf{s}, \quad (187)$$

where the real-space number density is:

$$n(\mathbf{r}) = \bar{n}[1 + \delta(\mathbf{r})], \quad (188)$$

and  $\delta(\mathbf{r})$  is the real-space density contrast. The volume elements are related by the Jacobian of the transformation  $\mathbf{s} = \mathbf{r} + \Delta\mathbf{r}$ :

$$d^3\mathbf{s} = \left| \frac{\partial \mathbf{s}}{\partial \mathbf{r}} \right| d^3\mathbf{r}, \quad (189)$$

$$d^3\mathbf{r} = \left| \frac{\partial \mathbf{r}}{\partial \mathbf{s}} \right| d^3\mathbf{s} = \left| \frac{\partial \mathbf{s}}{\partial \mathbf{r}} \right|^{-1} d^3\mathbf{s}. \quad (190)$$

Thus:

$$n_{\text{obs}}(\mathbf{s})d^3\mathbf{s} = n(\mathbf{r}) \left| \frac{\partial \mathbf{r}}{\partial \mathbf{s}} \right| d^3\mathbf{s}, \quad (191)$$

$$n_{\text{obs}}(\mathbf{s}) = n(\mathbf{r}) \left| \frac{\partial \mathbf{r}}{\partial \mathbf{s}} \right|. \quad (192)$$

Since  $\mathbf{r} = \mathbf{s} - \Delta\mathbf{r}$ :

$$n(\mathbf{r}) = n(\mathbf{s} - \Delta\mathbf{r}) = \bar{n}[1 + \delta(\mathbf{s} - \Delta\mathbf{r})], \quad (193)$$

$$n_{\text{obs}}(\mathbf{s}) = \bar{n}[1 + \delta(\mathbf{s} - \Delta\mathbf{r})] \left| \frac{\partial \mathbf{r}}{\partial \mathbf{s}} \right|. \quad (194)$$

The redshift-space density contrast is:

$$1 + \delta_{\text{obs}}(\mathbf{s}) = [1 + \delta(\mathbf{s} - \Delta\mathbf{r})] \left| \frac{\partial \mathbf{r}}{\partial \mathbf{s}} \right|. \quad (195)$$

## F.3 Jacobian Calculation

Compute the Jacobian matrix for the transformation:

$$s_x = r_x, \quad s_y = r_y, \quad s_z = r_z + \Delta r_i, \quad (196)$$

$$\Delta r_i = \frac{\beta \Delta C_i \Delta \phi_i}{H_0 c}. \quad (197)$$

The Jacobian matrix is:

$$\frac{\partial(s_x, s_y, s_z)}{\partial(r_x, r_y, r_z)} = \begin{pmatrix} 1 & 0 & 0 \\ 0 & 1 & 0 \\ \frac{\partial\Delta r_i}{\partial r_x} & \frac{\partial\Delta r_i}{\partial r_y} & 1 + \frac{\partial\Delta r_i}{\partial r_z} \end{pmatrix}. \quad (198)$$

Since  $\Delta r_i$  depends on  $\Delta\phi_i(\mathbf{r})$ :

$$\frac{\partial\Delta r_i}{\partial r_x} = \frac{\beta\Delta C_i}{H_0 c} \frac{\partial\Delta\phi_i}{\partial r_x}, \quad \frac{\partial\Delta r_i}{\partial r_y} = \frac{\beta\Delta C_i}{H_0 c} \frac{\partial\Delta\phi_i}{\partial r_y}, \quad \frac{\partial\Delta r_i}{\partial r_z} = \frac{\beta\Delta C_i}{H_0 c} \frac{\partial\Delta\phi_i}{\partial r_z}. \quad (199)$$

Assuming the potential gradient is primarily along the line-of-sight:

$$\frac{\partial\Delta r_i}{\partial r_x} \approx 0, \quad \frac{\partial\Delta r_i}{\partial r_y} \approx 0, \quad (200)$$

$$\frac{\partial\Delta r_i}{\partial r_z} = \frac{\beta\Delta C_i}{H_0 c} \frac{\partial\Delta\phi_i}{\partial z_i}. \quad (201)$$

The Jacobian matrix simplifies to:

$$\frac{\partial\mathbf{s}}{\partial\mathbf{r}} = \begin{pmatrix} 1 & 0 & 0 \\ 0 & 1 & 0 \\ 0 & 0 & 1 + \frac{\beta\Delta C_i}{H_0 c} \frac{\partial\Delta\phi_i}{\partial z_i} \end{pmatrix}. \quad (202)$$

The determinant is:

$$\left| \frac{\partial\mathbf{s}}{\partial\mathbf{r}} \right| = 1 + \frac{\beta\Delta C_i}{H_0 c} \frac{\partial\Delta\phi_i}{\partial z_i}. \quad (203)$$

The inverse Jacobian is:

$$\left| \frac{\partial\mathbf{r}}{\partial\mathbf{s}} \right| = \left( 1 + \frac{\beta\Delta C_i}{H_0 c} \frac{\partial\Delta\phi_i}{\partial z_i} \right)^{-1}. \quad (204)$$

Since the displacement is small ( $\frac{\beta\Delta C_i \Delta\phi_i}{c^2} \sim 10^{-5}$ ), approximate:

$$(1+x)^{-1} \approx 1-x, \quad x = \frac{\beta\Delta C_i}{H_0 c} \frac{\partial\Delta\phi_i}{\partial z_i}, \quad (205)$$

$$\left| \frac{\partial\mathbf{r}}{\partial\mathbf{s}} \right| \approx 1 - \frac{\beta\Delta C_i}{H_0 c} \frac{\partial\Delta\phi_i}{\partial z_i}. \quad (206)$$

#### F.4 Density Contrast Derivation

Substitute into the number conservation equation:

$$1 + \delta_{\text{obs}}(\mathbf{s}_i) = [1 + \delta(\mathbf{s}_i - \Delta\mathbf{r}_i)] \left( 1 - \frac{\beta\Delta C_i}{H_0 c} \frac{\partial\Delta\phi_i}{\partial z_i} \right). \quad (207)$$

Since  $\Delta\mathbf{r}_i$  is small, approximate:

$$\delta(\mathbf{s}_i - \Delta\mathbf{r}_i) \approx \delta(\mathbf{s}_i) - \Delta\mathbf{r}_i \cdot \nabla\delta(\mathbf{s}_i), \quad (208)$$



$$\Delta \mathbf{r}_i = \frac{\beta \Delta C_i \Delta \phi_i}{H_0 c} \hat{z}, \quad (209)$$

$$\Delta \mathbf{r}_i \cdot \nabla \delta(\mathbf{s}_i) = \frac{\beta \Delta C_i \Delta \phi_i}{H_0 c} \frac{\partial \delta(\mathbf{s}_i)}{\partial z_i}, \quad (210)$$

$$1 + \delta(\mathbf{s}_i - \Delta \mathbf{r}_i) \approx 1 + \delta(\mathbf{s}_i) - \frac{\beta \Delta C_i \Delta \phi_i}{H_0 c} \frac{\partial \delta(\mathbf{s}_i)}{\partial z_i}. \quad (211)$$

For the leading-order effect, focus on the Jacobian's contribution:

$$1 + \delta(\mathbf{s}_i - \Delta \mathbf{r}_i) \approx 1 + \delta(\mathbf{s}_i), \quad (212)$$

$$1 + \delta_{\text{obs}}(\mathbf{s}_i) \approx [1 + \delta(\mathbf{s}_i)] \left( 1 - \frac{\beta \Delta C_i}{H_0 c} \frac{\partial \Delta \phi_i}{\partial z_i} \right). \quad (213)$$

Expand, keeping first-order terms:

$$1 + \delta_{\text{obs}}(\mathbf{s}_i) \approx 1 + \delta(\mathbf{s}_i) - \frac{\beta \Delta C_i}{H_0 c} \frac{\partial \Delta \phi_i}{\partial z_i} - \delta(\mathbf{s}_i) \frac{\beta \Delta C_i}{H_0 c} \frac{\partial \Delta \phi_i}{\partial z_i}. \quad (214)$$

Neglect the second-order term:

$$\delta_{\text{obs}}(\mathbf{s}_i) \approx \delta(\mathbf{s}_i) - \frac{\beta \Delta C_i}{H_0 c} \frac{\partial \Delta \phi_i}{\partial z_i}. \quad (215)$$

Rewrite:

$$\delta_{\text{obs}}(\mathbf{s}_i) \approx \delta(\mathbf{s}_i) \left( 1 - \frac{\beta \Delta C_i}{H_0 c} \frac{\partial \Delta \phi_i}{\partial z_i} \right). \quad (216)$$

Relabel  $\mathbf{s}_i \rightarrow \mathbf{r}_i$ :

$$\delta_{\text{obs}}(\mathbf{r}_i) \approx \delta(\mathbf{r}_i) \left( 1 - \frac{\beta \Delta C_i}{H_0 c} \frac{\partial \Delta \phi_i}{\partial z_i} \right). \quad (217)$$

## F.5 Physical Interpretation

The term  $1 - \frac{\beta \Delta C_i}{H_0 c} \frac{\partial \Delta \phi_i}{\partial z_i}$  represents the volume correction due to the redshift-space mapping. A positive  $\frac{\partial \Delta \phi_i}{\partial z_i}$  indicates stretching of the real-space volume, reducing the observed density, while a negative gradient indicates compression, increasing the density.

## F.6 Assumptions

- Small displacements ( $\frac{\beta \Delta C_i \Delta \phi_i}{c^2} \ll 1$ ).
- Potential gradient primarily along the line-of-sight.
- First-order approximation in  $\beta$ .

## G Composition Difference $\Delta C$

The composition difference,  $\Delta C$ , quantifies differences in the physical properties of galaxy populations, such as the baryon-to-dark-matter ratio, stellar mass fraction, or gas content. For example, luminous red galaxies (LRGs) have a higher stellar mass and baryon-to-dark-matter ratio compared to emission-line galaxies (ELGs), which are gas-rich. We define:

$$\Delta C = \frac{(M_{\text{target}}/M_{\text{total}})}{(M_{\text{target}}/M_{\text{total}})_{\text{ref}}} - 1,$$

where  $M_{\text{target}}$  and  $M_{\text{total}}$  are the target testable and total masses, and the reference is a typical galaxy type.  $\Delta C$  is used to test WEP by checking if galaxies with different compositions follow the same gravitational trajectories.

### G.1 Compositional Difference on Baryon-Dark-Matter Ratio

We define:

$$\Delta C_{\text{Baryon-DM}} = \frac{(M_{\text{baryon}}/M_{\text{DM}})}{(M_{\text{baryon}}/M_{\text{DM}})_{\text{ref}}} - 1,$$

where  $M_{\text{baryon}}$  and  $M_{\text{DM}}$  are the baryonic and dark matter masses, and the reference is a typical galaxy type.

### G.2 Compositional Difference on Stellar-Mass Ratio

We define:

$$\Delta C_{\text{stellar}} = \frac{(M_{\text{stellar}}/M_{\text{total}})}{(M_{\text{stellar}}/M_{\text{total}})_{\text{ref}}} - 1,$$

where  $M_{\text{stellar}}$  and  $M_{\text{total}}$  are the stellar and total masses, and the reference is a typical galaxy type.

### G.3 Compositional Difference on Gas Fraction Ratio

We define:

$$\Delta C_{\text{gas}} = \frac{(M_{\text{gas}}/M_{\text{total}})}{(M_{\text{gas}}/M_{\text{total}})_{\text{ref}}} - 1,$$

where  $M_{\text{gas}}$  and  $M_{\text{total}}$  are the gas and total masses, and the reference is a typical galaxy type.

### G.4 Estimation of $\Delta C = \Delta C_2 - \Delta C_1$

The parameter is defined as:

$$\Delta C_{\text{Baryon-DM},i} = \frac{(M_{\text{baryon}}/M_{\text{DM}})_i}{(M_{\text{baryon}}/M_{\text{DM}})_{\text{ref}}} - 1.$$

Assume the reference ratio is the cosmic mean:

$$(M_{\text{baryon}}/M_{\text{DM}})_{\text{ref}} = 0.16.$$

For Galaxy 1 (spiral), with  $\frac{M_{\text{baryon}}}{M_{\text{DM}}} = 0.1$ :

$$\Delta C_1 = \frac{0.1}{0.16} - 1 = 0.625 - 1 = -0.375.$$

For Galaxy 2 (elliptical), with  $\frac{M_{\text{baryon}}}{M_{\text{DM}}} = 0.05$ :

$$\Delta C_2 = \frac{0.05}{0.16} - 1 = 0.3125 - 1 = -0.6875.$$

The difference is:

$$\Delta C = \Delta C_2 - \Delta C_1 = -0.6875 - (-0.375) = -0.3125.$$

## H Table of Symbols

Below is a table of all symbols used in this document, organized alphabetically for easy reference. See Tables 1 and 2.

Symbol	Meaning
<i>Greek Letters</i>	
$\alpha$	Parameter for LPI violation
$\beta$	Parameter for WEP violation
$\gamma$	Parameter for LLI violation
$\Delta C$	Composition difference
$\delta$	Density contrast
$\delta z$	Composition-dependent redshift contribution
$\xi(s, \mu)$	2-point correlation function
$\xi_0(s)$	Monopole term of the correlation function
$\xi_1(s)$	Dipole term of the correlation function
$\mu$	Cosine of the angle between separation vector and line of sight
$\sigma_v$	Velocity dispersion
$\phi$	Gravitational potential

**Table 1** Table of symbols used in this document.

Symbol	Meaning
<i>Latin Letters</i>	
$A$	Normalization constant
$c$	Speed of light
$d$	Comoving distance
$d_A$	Angular diameter distance
$d_M$	Proper motion distance
$d_H$	Hubble distance
$G$	Gravitational constant
$H_0$	Hubble constant
$j_0(ks)$	Spherical Bessel function of order 0
$k$	Wavenumber
$k_{\text{BAO}}$	BAO scale
$k_{\text{pivot}}$	Pivot scale
$M_{\text{baryon}}$	Baryonic mass
$M_{\text{DM}}$	Dark matter mass
$M_{\text{gas}}$	Gas mass
$M_{\text{halo}}$	Halo mass
$M_{\text{stellar}}$	Stellar mass
$M_{\text{target}}$	Target testable mass
$M_{\text{total}}$	Total mass
$n_s$	Spectral index
$P(k)$	Power spectrum
$P_l(\mu)$	Legendre polynomials
$P_m(k)$	Matter power spectrum
$s$	Separation distance
$v_{\text{pec}}$	Peculiar velocity
$v_{\text{rel}}$	Relative velocity
$z$	Redshift
$z_{\text{cosmo}}$	Cosmological redshift
$z_{\text{Doppler}}$	Doppler redshift
$z_{\text{grav}}$	Gravitational redshift
$z_{\text{LLI}}$	LLI-violating redshift
$z_{\text{LPI}}$	LPI-violating redshift
$z_{\text{obs}}$	Observed redshift
$z_{\text{WEP}}$	WEP-violating redshift
$\langle v_{\text{rel}} \rangle$	Average relative velocity
$\chi^2$	Chi-square statistic

**Table 2** Table of symbols used in this document.